© 2016. Published by The Company of Biologists Ltd | Development (2016) 143, 4352-4367 doi:10.1242/dev.136879

STEM CELLS AND REGENERATION

RESEARCH ARTICLE

Specification of osteoblast cell fate by canonical Wnt signaling requires *Bmp2*

Valerie S. Salazar[1], Satoshi Ohte[1,2], Luciane P. Capelo[1,3], Laura Gamer[1] and Vicki Rosen[1,*]

ABSTRACT

Enhanced BMP or canonical Wnt (cWnt) signaling are therapeutic strategies employed to enhance bone formation and fracture repair, but the mechanisms each pathway utilizes to specify cell fate of bone-forming osteoblasts remain poorly understood. Among all BMPs expressed in bone, we find that singular deficiency of *Bmp2* blocks the ability of cWnt signaling to specify osteoblasts from limb bud or bone marrow progenitors. When exposed to cWnts, *Bmp2*-deficient cells fail to progress through the *Runx2*/*Osx1* checkpoint and thus do not upregulate multiple genes controlling mineral metabolism in osteoblasts. Cells lacking *Bmp2* after induction of *Osx1* differentiate normally in response to cWnts, suggesting that pre-*Osx1*$^{+}$ osteoprogenitors are an essential source and a target of BMP2. Our analysis furthermore reveals Grainyhead-like 3 (Grhl3) as a transcription factor in the osteoblast gene regulatory network induced during bone development and bone repair, which acts upstream of *Osx1* in a BMP2-dependent manner. The *Runx2*/*Osx1* transition therefore receives crucial regulatory inputs from BMP2 that are not compensated for by cWnt signaling, and this is mediated at least in part by induction and activation of Grhl3.

KEY WORDS: BMP, Wnt, Osteoblast, Osx1, Sp7, Dlx5, Grhl3, Mouse MLB13 cells

INTRODUCTION

Bone morphogenetic proteins (BMPs) and canonical Wnts (cWnts) play essential roles in the skeleton. BMPs, originally identified for their ability to induce *de novo* formation of bone and cartilage, are secreted ligands that act through cell surface complexes comprised of type I and type II BMP receptors to activate Smad1/5/8-dependent gene transcription (Salazar et al., 2016). cWnts are secreted proteins that signal through Lrp and Frizzled co-receptor complexes to stabilize intracellular pools of β-catenin and activate Tcf/Lef-dependent gene transcription (Baron and Kneissel, 2013). Genetic mutations in either of these pathways underlie a variety of severe skeletal pathologies including the high and low bone mass syndromes associated with mutations of the cWnt receptor Lrp5 (Boyden et al., 2002; Gong et al., 2001; Little et al., 2002) or fibrodysplasia ossificans progressiva, a disease characterized by inappropriate growth of endochondral bone at non-skeletal sites and caused by mutations of the type I BMP receptor ALK2 (Shore et al., 2006). For over a decade, recombinant BMPs, particularly BMP2 and BMP7, have been used in clinical orthopedic settings including non-union fractures, spinal fusions and oral surgery (Lo et al., 2012). More recently, neutralizing antibodies targeting antagonists of the cWnt pathway, such as SOST and DKK1, have entered clinical trials as systemic agents that enhance bone formation (Baron and Kneissel, 2013).

Given the abundance of information establishing clear roles for BMP and cWnt signaling in bone development and disease, and the fact that therapies based on each pathway are approved or under evaluation for use in humans, it is somewhat remarkable that the individual aspects of osteoblast specification and physiology controlled by either BMP or cWnt signaling remain largely undefined.

During development, bones of the appendicular skeleton are made by a *Prx1* (*Prrx1*)$^{+}$ subset of cells that arise in lateral plate mesoderm during limb bud outgrowth (Durland et al., 2008; Logan et al., 2002). Postnatally, undifferentiated cells of the *Prx1* lineage persist in the marrow and periosteum of mature bone as distinct but complementary pools of *Lepr*$^{+}$ or *Grem1*$^{+}$ osteoprogenitors that can be activated by BMP2 for the purpose of bone growth or repair (Chan et al., 2015; Worthley et al., 2015; Zhou et al., 2014). We hypothesized that BMPs and cWnts play unique roles in specifying *Prx1*$^{+}$ progenitors to the osteoblast cell fate. To test this, we utilized limb bud cells and bone marrow cells as models of *Prx1*$^{+}$ cell populations to monitor osteogenic responses to cWnt activity in the presence or absence of *Bmp2*.

RESULTS

Bmp2 is required for limb bud cells to undergo osteoblast differentiation in response to Wnt3a

Immortalized cells from the E13.5 mouse embryonic limb bud (MLB13 cells) express endogenous *Bmp2* and exhibit robust endochondral differentiation in response to recombinant BMPs (Rosen et al., 1993, 1994). We established a sub-clonal population of MLB13 (MLB13^{WT}) cells stably expressing siRNA against endogenous *Bmp2* (MLB13^{kdBmp2}) (Fig. 1A). Osteoblast differentiation was induced for 48 h by supplementing the cell culture medium with ascorbic acid and β-glycerophosphate (osteogenic medium) with or without recombinant (r)BMP2 or Wnt3a. QPCR analysis revealed that levels of *Prx1*, *Runx2* and *Dlx5* mRNA were unaffected by knockdown of *Bmp2*, while *Osx1* (*Sp7*) and the direct transcriptional target of Osx1, *Alpl* (Hojo et al., 2016), were dramatically diminished. *Osx1* and *Alpl* mRNAs could be enhanced in MLB13^{kdBmp2} cells by rBMP2 but not rWnt3. Wnt3a furthermore significantly diminished *Dlx5* mRNA in MLB13^{kdBmp2} but not MLB13^{WT} cells (Fig. 1B-F). MLB13^{kdBmp2} cells treated with Wnt3a retained the ability to

[1]Department of Developmental Biology, Harvard School of Dental Medicine, 188 Longwood Avenue, Boston, MA 02115, USA. [2]Division of Pathophysiology, Research Center for Genomic Medicine, Saitama Medical University, 1397-1 Yamane, Hidaka-shi, Saitama 350-1241, Japan. [3]Instituto de Ciência e Tecnologia, Universidade Federal de São Paulo, Rua Talim, 330, São José dos Campos, São Paulo, CEP 12231-280, Brazil.

*Author for correspondence (Vicki_Rosen@hsdm.harvard.edu)

V.S.S., 0000-0002-2111-9313; S.O., 0000-0002-5153-2176; L.P.C., 0000-0002-3004-1220; L.G., 0000-0002-1324-2741; V.R., 0000-0002-4029-1055

Received 18 March 2016; Accepted 7 October 2016

Development (2016) 143, 4352-4367 doi:10.1242/dev.136879

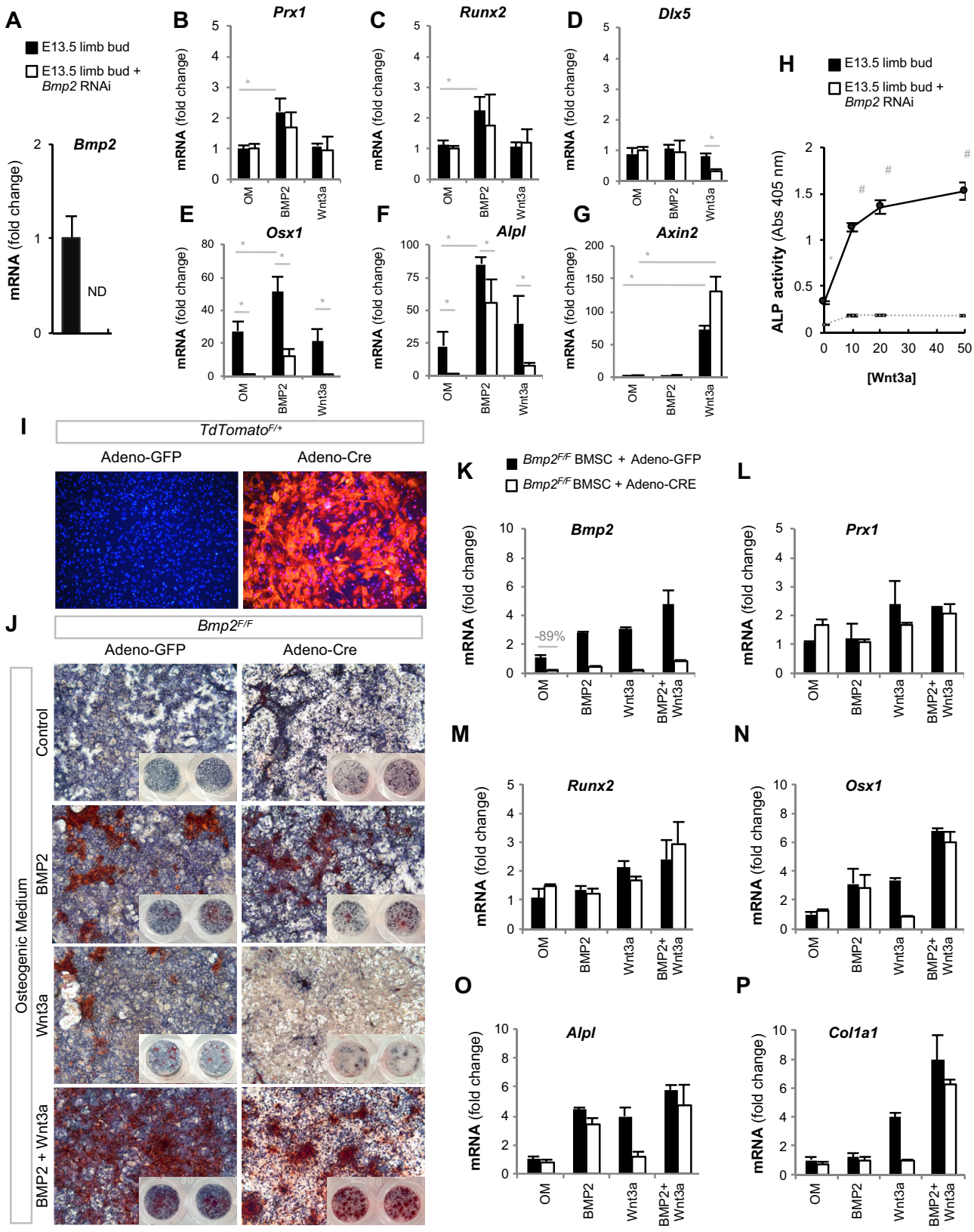

Fig. 1. See next page for legend.

upregulate the TCF/Lef target gene *Axin2* (Fig. 1G). MLB13^{WT} cells exhibited a dose-dependent increase in ALP activity in response to Wnt3a, whereas ALP activity in MLB13^{kdBmp2} cells was ~73% lower than MLB13^{WT} cells grown in osteogenic medium alone and remained unchanged by any concentration of Wnt3a (Fig. 1H).

Development (2016) 143, 4352-4367 doi:10.1242/dev.136879

Fig. 1. Lack of *Bmp2* in limb bud or bone marrow stromal cells blocks osteoblast differentiation in response to Wnt3a. (A-H) Immortalized mouse limb bud cells from E13.5 embryos (MLB13^{WT} cells) were transfected with plasmid-based shRNA to establish a clonal population of cells with stable knockdown of *Bmp2* (MLB13^{kdBmp2} cells). (A-G) QPCR, expressed as mean fold change relative to MLB13^{WT} cells. *N*=3 biological replicates, **P*<0.05. (H) Alkaline phosphatase activity in MLB13 cells cultured for 48 h with increasing concentrations of Wnt3a. *N*=3 biological replicates; **P*<0.05 vs control MLB13^{kdBmp2} cells. $^{\#}$*P*<0.05 vs control MLB13^{WT} cells. (I) Primary bone marrow stromal cells (BMSCs) from *TdTomato*$^{flox\text{-}stop\text{-}flox/+}$ mice were transduced with Adeno-GFP or Adeno-Cre. The efficiency of transduction and recombination was visualized by DAPI and RFP filters (10×, fluorescence). (J-P) BMSCs from *Bmp2*$^{F/F}$ mice were transduced with Adeno-GFP or Adeno-Cre and differentiated in osteogenic medium (OM) plus recombinant growth factors. (J) Alkaline phosphatase activity (blue) and matrix calcification (red) was assessed by biochemical staining on day 10 (2.5×, brightfield, with 1× inset). (K-P) QPCR analysis, expressed as mean fold change relative to *Bmp2*$^{F/F}$+Adeno-Cre cells grown in osteogenic medium alone. Error bars represent s.d. of two independent experiments.

Bmp2 is required for bone marrow stromal cells to form osteoblasts and mineralize matrix in response to Wnt3a

We also examined Wnt-induced osteoblast differentiation of adult bone marrow stromal cells (BMSCs) lacking *Bmp2* expression. BMSCs carrying a single copy of the *TdTomato*$^{Flox\text{-}stop\text{-}Flox}$ reporter allele were used to optimize a protocol for *in vitro* recombination using Adeno-Cre. Fluorescence microcopy showed that nearly all *TdTomato*$^{Flox\text{-}stop\text{-}Flox}$ cells transduced with Adeno-Cre but none of the cells transduced with Adeno-GFP were Tomato^{+} (Fig. 1I). BMSCs carrying two floxed alleles of *Bmp2* (*Bmp2*$^{F/F}$) were transduced with Adeno-GFP (*Bmp2*$^{AdenoF/F}$) or Adeno-Cre (*Bmp2*$^{AdenoΔ/Δ}$), and osteoblast differentiation was induced with osteogenic medium with or without BMP2 or Wnt3a. After 10 days, BMSCs were stained with alkaline phosphatase (ALP) substrate to monitor induction of osteoblast differentiation and Alizarin Red dye to visualize calcification of the extracellular matrix. ALP activity and matrix calcification were comparable in *Bmp2*$^{AdenoF/F}$ and *Bmp2*$^{AdenoΔ/Δ}$ cells grown in control osteogenic conditions, enhanced in both genotypes of cells by rBMP2, and were greatest in both genotypes of cells treated with BMP2 and Wnt3a. By contrast, Wnt3a enhanced ALP activity and matrix calcification of *Bmp2*$^{AdenoF/F}$ cells but not *Bmp2*$^{AdenoΔ/Δ}$ cells, which exhibited even less osteoblast differentiation in response to Wnt3a than cells grown in osteogenic medium alone (Fig. 1J). BMSCs were analyzed on day 7 by QPCR to confirm recombination of *Bmp2* (Fig. 1K) and assess osteoblast markers. Similar to results obtained in limb bud cells, mRNAs for *Prx1* and *Runx2* were not diminished by loss of *Bmp2*, while *Osx1* and two Osx1 target genes, *Alpl* and *Col1a1* (Hojo et al., 2016), were significantly reduced in *Bmp2*$^{AdenoΔ/Δ}$ cells exposed to Wnt3a (Fig. 1L-P).

Canonical Wnt signaling does not compensate for selective ablation of *Bmp2* in *Prx1*$^{+}$ cells

Prx1-Cre was used to conditionally delete *Bmp2* in the limb bud mesenchyme at E9.5 when endochondral progenitors of the appendicular skeleton first appear during development (Durland et al., 2008; Logan et al., 2002). *Bmp2* was efficiently ablated by endogenous expression of *Prx1-Cre*, was expressed in *Bmp2*$^{F/F}$ BMSC and was upregulated by BMP2, Wnt3a and BMP2+Wnt3a together (Zhang et al., 2013) (Fig. 2A). Osteoblast lineage markers including *Prx1*, *Runx2*, *Osx1*, *Alpl* and *Col1a1* were upregulated in *Bmp2*$^{F/F}$ cells treated with BMP2 or Wnt3a, and most strongly expressed in *Bmp2*$^{F/F}$ cells treated with BMP2 plus Wnt3a. These genes were also upregulated in *Bmp2*$^{Prx1Δ/Δ}$ cells treated with BMP2 or BMP2 plus Wnt3a, to levels comparable to those in wild-type (WT) cells grown under corresponding conditions. However, with the exception of *Prx1 and Runx2*, *Bmp2*$^{Prx1Δ/Δ}$ cells treated with Wnt3a did not upregulate the osteoblast differentiation markers *Osx1*, *Alpl* and *Col1a1* to similar levels as observed in *Bmp2*$^{F/F}$ cells (Fig. 2B-F). BMSCs from *Bmp2*$^{F/F}$ or *Bmp2*$^{Prx1Δ/Δ}$ mice produced comparable levels of calcified matrix (Fig. 2G,H) and immunoblot analysis showed they expressed similar amounts of Osx1 protein (Fig. 2I). BMP2 greatly enhanced matrix mineralization (Fig. 2G,H) and the abundance of Osx1 in *Bmp2*$^{F/F}$ or *Bmp2*$^{Prx1Δ/Δ}$ cells (Fig. 2I), confirming our *in vivo* observation that osteoprogenitors in *Bmp2*$^{Prx1Δ/Δ}$ mice retain the ability to respond to exogenous BMP2 (Chappuis et al., 2012). In stark contrast, Wnt3a greatly enhanced the amount of mineralized matrix and Osx1 protein produced by WT cells but not by *Bmp2*$^{Prx1Δ/Δ}$ cells (Fig. 2G-I), which made even less mineralized matrix and Osx1 protein than *Bmp2*$^{Prx1Δ/Δ}$ cells grown in osteogenic medium alone (Fig. 2G, control). Concomitant treatment of cells with both BMP2 and Wnt3a also induced robust mineralization and Osx1 expression (Fig. 2G-I). Notably, this response was indistinguishable between WT and *Bmp2*$^{Prx1Δ/Δ}$ cells, indicating that the ability of *Bmp2*$^{Prx1Δ/Δ}$ cells to upregulate Osx1 and make calcified matrix in the presence of Wnt3a is fully rescued by exogenous BMP2. The Osx1 banding pattern in cells treated with BMP2 and/or Wnt3a was complex, with the appearance of several slower-migrating bands, suggesting that Osx1 undergoes post-translational modifications in differentiating osteoblasts, as seen with other Sp transcription factor family members (Waby et al., 2008). Regardless of culture supplements, *Bmp2*$^{Prx1Δ/Δ}$ BMSCs had reduced levels of phosphorylated Smad1/5 but similar levels of phosphorylated Smad2/3 compared with *Bmp2*$^{F/F}$ BMSCs, suggesting that total BMP signaling was reduced while TGF-β/activin signaling remained unchanged (Fig. 2I).

Bmp2-deficient cells are able to activate Tcf/Lef-dependent transcription

We further examined the possibility that diminished osteogenic response of *Bmp2*$^{Prx1Δ/Δ}$ cells to Wnt3a can be explained by an inability of *Bmp2*-deficient cells to activate Tcf/Lef activity. Immunoblots revealed that β-catenin, an essential transcriptional mediator of cWnt signaling, was modestly reduced in *Bmp2*$^{Prx1Δ/Δ}$ cells and markedly diminished in *Bmp2*$^{Prx1Δ/Δ}$ cells treated with Wnt3a (Fig. S1A). QPCR showed that mRNAs encoding essential signaling molecules of the cWnt pathway are expressed in *Bmp2*$^{Prx1Δ/Δ}$ cells grown in osteogenic medium with or without Wnt3a (Fig. S1B), as well as *Bmp2*$^{AdenoΔ/Δ}$ cells grown in osteogenic medium with or without Wnt3a (Fig. S1C), suggesting that the diminished amounts of β-catenin protein detected in *Bmp2*$^{Prx1Δ/Δ}$ cells grown with or without Wnt3a (Fig. S1A) occurs via a post-transcriptional mechanism. Despite diminished protein levels of β-catenin in *Bmp2*$^{Prx1Δ/Δ}$ cells, the Tcf/Lef-target gene *Axin2* (Jho et al., 2002) was strongly upregulated in *Bmp2*$^{Prx1Δ/Δ}$ cells (Fig. S2B) or *Bmp2*$^{AdenoΔ/Δ}$ cells following exposure to Wnt3a (Fig. S2C), similar to previous results obtained in MLB13 cells (Fig. 1G).

Wnt3a induces a different transcriptome in *Bmp2*$^{F/F}$ and *Bmp2; Prx1-Cre* cells

We next performed comparative transcriptome-level gene expression analysis. BMSCs from *Bmp2*$^{F/F}$ or *Bmp2*$^{Prx1Δ/Δ}$ mice were differentiated with osteogenic medium alone, BMP2, Wnt3a or BMP2+Wnt3a. RNA was harvested on day 7 to generate 24 samples. All 24 samples were used to prepare cDNA for traditional QPCR analysis. A subset of samples was also used to make cDNA

Development (2016) 143, 4352-4367 doi:10.1242/dev.136879

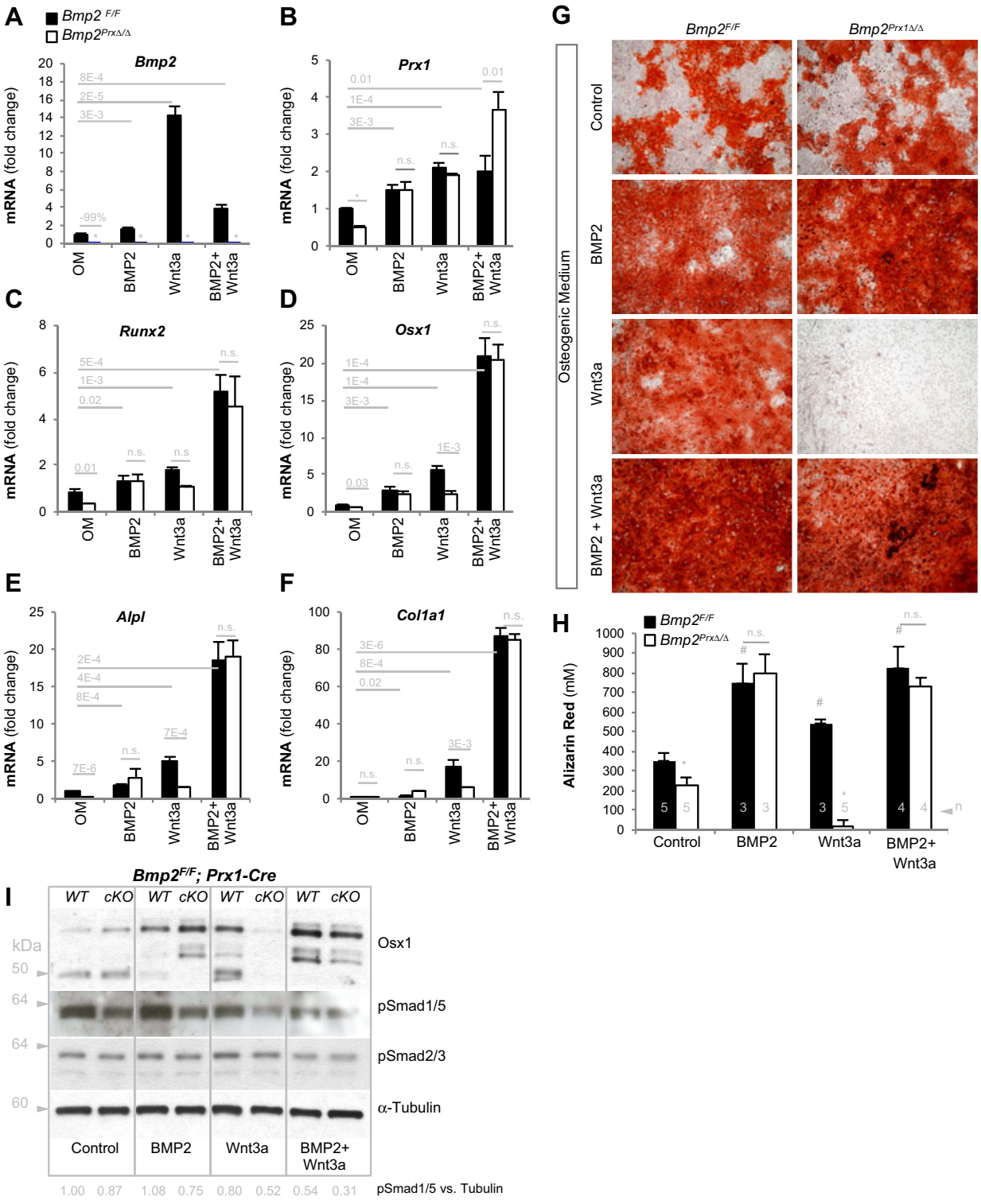

Fig. 2. Conditional ablation of *Bmp2* in the *Prx1*$^{+}$ lineage blocks osteoblast activity in response to cWnt signaling. Primary BMSCs were collected from *Bmp2*$^{Flox/Flox}$ (*Bmp2*$^{F/F}$) or *Bmp2; Prx1-Cre* (*Bmp2*$^{Prx1\Delta/\Delta}$) mice and induced with osteogenic medium (OM) plus recombinant growth factors. (A) Calcified matrix was assessed by Alizarin Red staining on day 10 (2.5×, bright field). (B) Quantification of Alizarin Red; mean±s.d. **P*<0.001 vs *Bmp2*$^{F/F}$ cells grown in corresponding condition. $^{\#}$*P*<0.001 vs *Bmp2*$^{F/F}$ cells grown in osteogenic medium (OM). *N*, number of cultures. (C) SDS-PAGE and immunoblot on RIPA lysates from day 7. Images are representative of two experiments. (D-I) QPCR on biological triplicates harvested on day 7, expressed as mean fold change±s.d. from *N*=3 biological replicates.

libraries for microarray analysis: (1) one pooled sample of *Bmp2*$^{F/F}$ extracts (*n*=3); (2) three unpooled samples of *Bmp2*$^{F/F}$+Wnt3a extracts; (3) three unpooled samples *Bmp2*$^{Prx1\Delta/\Delta}$+Wnt3a extracts; and (4) one pooled sample of *Bmp2*$^{Prx1\Delta/\Delta}$ cells treated with BMP2+Wnt3a (*n*=3). All eight samples performed as a single tissue type (Fig. S2A), had similar gene-level mean signal intensities after normalization and summarization using Expression Console (Fig. S2B) and produced a >2-fold signal to background ratio

Development (2016) 143, 4352-4367 doi:10.1242/dev.136879

(Fig. S2C). Pearson's correlation analysis demonstrated that the four sample types segregated into four distinct groups according to genotype and treatment (Fig. S2D).

Gene expression was calculated as linear fold change in $Bmp2^{F/F}$ relative to $Bmp2^{Prx1\Delta/\Delta}$ cells treated with Wnt3a. When the top 5000 most differentially regulated genes were used to perform hierarchical cluster analysis, samples from $Bmp2^{F/F}$ or $Bmp2^{Prx1\Delta/\Delta}$ cells treated with Wnt3a segregated into two distinct groups based on genotype (Fig. 3A). A total of 165 genes were downregulated >2 fold in $Bmp2^{F/F}$ versus $Bmp2^{Prx1\Delta/\Delta}$ (blue datapoints, Fig. 3B) and 114 genes were upregulated >2 fold in $Bmp2^{F/F}$ versus $Bmp2^{Prx1\Delta/\Delta}$ (red datapoints, Fig. 3B), where $P<0.05$. Differentially regulated genes were widely distributed throughout the genome and every chromosome (Fig. 3C).

The Runx2/Osx1 transition and induction of mineral metabolism requires expression of *Bmp2* in the *Prx1*$^+$ lineage and is not compensated for by cWnt signaling

We identified several pathways with ≥2 targets exhibiting ≥2-fold change in expression and a *P*-value ≤0.05 (Fig. 3D). Consistent with a study focused on cells lacking *Bmp2*, molecules in the BMP pathway, including *Bmp2*, and transcriptional gene targets of BMP signaling, including *Smad6*, *Smad8*, *Id1* and *Id3* (Table 1) were enriched. Intriguingly, the phenotype of $Bmp2^{Prx1\Delta/\Delta}$ cells remains despite the fact that BMSC-derived osteoblasts expressed ≥17 other BMP/GDF ligands, and a variety of Type I and Type II BMP receptors that is sufficient to maintain some BMP signaling (Table 1 and Fig. 2I). Several modulators of Wnt signaling were altered in $Bmp2^{Prx1\Delta/\Delta}$ cells treated with Wnt3a, including *Lgr5*, *Lgr6*, *Wif1*, *Notum*, and *Sfrp2*; however, many established Tcf/Lef target genes, including *Axin2* and *Lef1*, were induced normally following exposure to Wnt3a, confirming that cWnt signaling was functional in the absence of *Bmp2* (Table 2). Consistent with the mesenchymal and stem/progenitor cell nature of input samples, targets related to pluripotency, endochondral ossification and adipogenesis pathways were enriched (Fig. 3D) and included *Lifr*, *FGFR2*, *Ihh*, *Ptch1*, *Mef2c* and *Sox9* (Table 3). $Bmp2^{Prx1\Delta/\Delta}$ cells treated with Wnt3a expressed early markers of endochondral lineages, but expressed statistically low levels of *Osx1*, *Dlx3* and *Dlx5* (Table 3). A variety of G-protein-coupled receptors with established roles in osteoblasts were also enriched, including serotonin receptor type 2a (*Htr2a*) and *Pthr1* (*Pth1r*). $Bmp2^{Prx1\Delta/\Delta}$ cells treated with Wnt3a do not mineralize, and indeed these cells fail to induce *Alpl* and *Phospho1*, which are both poly-phosphate-metabolizing enzymes required during development for mineralization of the skeleton (Yadav et al., 2011), and *Dmp1*, a glycoprotein involved in bone/renal mineral homeostasis (Rowe, 2012) (Table 4). BMSC-derived osteoblasts expressed all 15 members of the carbonic anhydrase family – enzymes recently implicated in production of precursors to mature calcium hydroxyapatite crystals of vertebrate bone (Müller et al., 2013; Wang et al., 2014); $Bmp2^{Prx1\Delta/\Delta}$ cells treated with Wnt3a expressed negligible levels of both *Car3* and *Car12* (Table 4).

QPCR was used to validate selected genes identified by microarray and furthermore evaluate their expression profiles in cells treated with BMP2 or BMP2 plus Wnt3a. As previously reported, *Bmp2* and *Bmp4* were upregulated by Wnt3a in $Bmp2^{F/F}$ cells (Shu et al., 2005; Zhang et al., 2013) (Fig. 4A). $Bmp2^{F/F}$ and $Bmp2^{Prx1\Delta/\Delta}$ cells expressed similar levels of early endochondral lineage markers *Prx1* and *Runx2*, but $Bmp2^{Prx1\Delta/\Delta}$ cells treated with Wnt3a failed to acquire a committed osteoblast phenotype characterized by increased expression of *Osx1*, *Dlx3* and *Dlx5* (Fig. 4B). $Bmp2^{F/F}$ and $Bmp2^{Prx1\Delta/\Delta}$ cells expressed similar levels of *Alpl* and *Phospho1*, *Car3*, *Car12* and *Dmp1*, but $Bmp2^{Prx1\Delta/\Delta}$ cells treated with Wnt3a expressed only modest levels of these genes (Fig. 4B). Expression of osteoblast markers and mineral metabolism enzymes in $Bmp2^{Prx1\Delta/\Delta}$ cells treated with Wnt3a could be rescued by complementation with exogenous BMP2 (Fig. 4B,C). In this experiment, the fundamental finding that *Bmp2*-deficient cells exhibit impaired progression to the *Osx1/Dlx5*$^+$ cell fate phenotype in response to Wnt3a was clear; however, some responses to BMP2 were blunted, presumably as a result of a weak batch of BMP2. We therefore cultured primary BMSCs one more time, and used QPCR to verify that $Bmp2^{Prx1\Delta/\Delta}$ cells are unable to induce *Osx1* in response to Wnt3 without complementation by exogenous BMP2 (Fig. 4D). These samples were used to proceed with analysis of *Grhl3*, one of the most highly altered genes identified by comparative microarray analysis on $Bmp2^{Prx1\Delta/\Delta}$ cells treated with Wnt3a.

Grhl3 encodes a transcription factor not previously recognized to play a role in osteoblast cell fate specification. In BMSCs, *Grhl3* expression was induced by Wnt3a >50-fold in $Bmp2^{Prx1\Delta/\Delta}$ cells and >117-fold in $Bmp2^{F/F}$ cells. *Grhl3* expression was not induced at the mRNA level by BMP2 alone, but was maximally induced (>300-fold) regardless of genotype in BMSCs co-stimulated with BMP2 and Wnt3a (Fig. 4E). In MLB13 cells, *Grhl3* mRNA was diminished by knockdown of *Bmp2*, and enhanced by Wnt3a regardless of the *Bmp2* genotype (Fig. 4F). The USCS Genome Browser (Kent et al., 2002) was used to examine the genetic locus of murine *Grhl3* (Fig. S3A) and revealed two consensus Tcf/Lef-binding sites (Cadigan and Waterman, 2012; Frietze et al., 2012; Guenther et al., 2014) in regions of high to medium genomic conservation in vertebrates (Fig. S3B,C). Compared with MLB13 cells expressing plasmid-derived EGFP, *Grhl3* mRNA was increased 12 h after transfection by a plasmid encoding Wnt1, but not by a plasmid encoding Wnt5. *Grhl3* was also induced by 4 h of treatment with recombinant Wnt3a, and this induction was not sensitive to increasing titrations of cycloheximide (25-100 µg/ml), suggesting that protein translation is not required for *Grhl3* induction by cWnt signaling (Fig. 4G) and that *Grhl3* is a direct canonical Wnt target gene.

Bmp2 is dispensable after acquisition of *Osx1*$^+$ cell fate for osteoblast differentiation and mineralization

To examine the relevance of our microarray analysis, we first tested the model that *Bmp2* is required at the *Runx2/Osx1* transition during Wnt-activated differentiation of osteoblasts. Mice were bred to conditionally ablate *Bmp2* in committed *Osx1*$^+$ osteoblasts ($Bmp2^{F/F}$; *Osx1-GFP::Cre* or $Bmp2^{Osx1\Delta/\Delta}$) using the *Osx1-GFP::Cre* transgene (Rodda and McMahon, 2006). BMSCs were cultured in osteogenic medium with BMP2, Wnt3a or BMP2 plus Wnt3a. Alizarin Red staining revealed that $Bmp2^{F/F}$ cells had partially mineralized their matrix; this was enhanced by treatment with either BMP2 or Wnt3a; and mineralization was maximized by dual exposure to BMP2 plus Wnt3a (Fig. 5A, left panels and B). $Bmp2^{Osx1\Delta/\Delta}$ cells produced comparable levels of mineralized matrix under each corresponding culture condition, including after Wnt3a exposure (Fig. 5A, right panels and B). QPCR analysis on RNA from day 7 confirmed that Osx1-Cre had successfully recombined *Bmp2* in $Bmp2^{Osx1\Delta/\Delta}$ cells (Fig. 5C). Furthermore, *Prx1*, *Runx2*, *Osx1*, *Dlx3* and *Dlx5* levels were indistinguishable between $Bmp2^{F/F}$ and $Bmp2^{Osx1\Delta/\Delta}$ cells for each condition (Fig. 5D). And, consistent with results from Alizarin Red

Development (2016) 143, 4352-4367 doi:10.1242/dev.136879

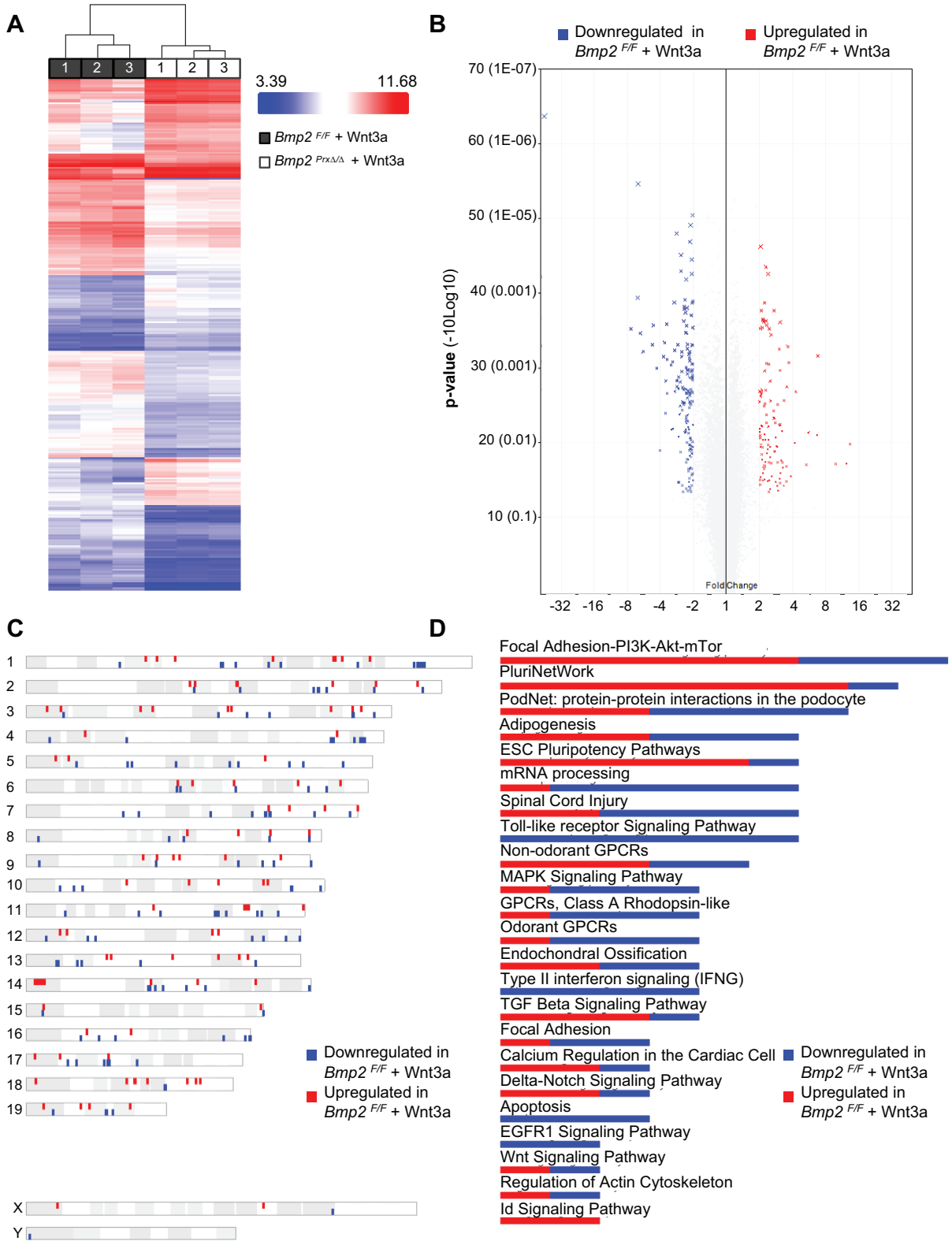

Fig. 3. Microarray analysis reveals that *Bmp2*$^{F/F}$ or *Bmp2; Prx1-Cre* cells produce a differential gene expression signature when stimulated with Wnt3a. Primary BMSCs were differentiated in osteogenic medium (OM) plus Wnt3a. Cultures were performed in biological triplicates using pooled cells from n=3 *Bmp2*$^{F/F}$ or n=4 *Bmp2*$^{Prx1\Delta/\Delta}$ mice. RNA was harvested on day 7 and analyzed by microarray. (A) Hierarchical cluster analysis comparing the 5000 most differentially regulated genes. (B) Volcano plot where gene expression is calculated as linear fold change relative to *Bmp2*$^{Prx1\Delta/\Delta}$ cells treated with Wnt3a, and P-value is calculated by one-way between-subject ANOVA for unpaired samples. Blue data points represent genes expressed >2-fold less and red data points represent genes expressed >2-fold more in *Bmp2*$^{F/F}$ versus *Bmp2*$^{Prx1\Delta/\Delta}$, where P<0.05. (C) Genomic distribution of differentially regulated genes is displayed relative to chromosomal location. (D) WikiPathway analysis identified pathways with at least two genes exhibiting a ≥2-fold change in expression with P≤0.05.

Development (2016) 143, 4352-4367 doi:10.1242/dev.136879

Table 1. Summary of microarray data assessing expression of genes in the BMP signaling pathway in *Bmp2*$^{F/F}$ or *Bmp2*$^{Prx1\Delta/\Delta}$ cells treated with Wnt3a

Gene	Fold change *Bmp2*$^{F/F}$+Wnt3a vs *Bmp2*$^{F/F}$)	*P*-value (ANOVA, unpaired)	Fold change (*Bmp2*$^{Prx1\Delta/\Delta}$ +Wnt3a vs *Bmp2*$^{F/F}$ +Wnt3a)	*P*-value (ANOVA, unpaired)
Bmp2	2.64	0.002	−2.16	0.026
Bmp3	1.4	0.007	1.03	0.963
Bmp4	1.18	0.043	−1.17	0.515
Bmp5	1.05	0.495	−1.61	0.007
Bmp6	1.03	0.854	−1.13	0.459
Bmp7	1.01	0.894	−1.21	0.009
Bmp8b	1.02	0.796	1	0.886
Bmp10	1.1	0.181	−1.14	0.071
Gdf1	−1.02	0.606	−1.02	0.621
Gdf2	−1.09	0.006	−1.17	0.016
Gdf3	1.49	0.083	1.12	0.903
Gdf5	−1.02	0.747	1.05	0.606
Gdf6	2.5	0.175	2.35	0.006
Gdf7	1.4	0.044	2.44	0.0002
Gdf9	1.01	0.576	−1.03	0.109
Gdf10	1.04	0.642	−1.11	0.152
Gdf15	1.23	0.074	−1.26	0.069
Gdf11	1.11	0.296	−1.04	0.277
Bmpr1a	−1.12	0.077	−1.16	0.103
Bmpr1b	1.05	0.326	1.15	0.087
Bmpr2	1.16	0.098	−1.06	0.389
Acvr2a	1.25	0.176	−1.02	0.164
Acvr2b	1.07	0.879	−1.06	0.460
Noggin	−1.45	0.011	−1.38	0.11
Grem1	3.03	0.008	−1.22	0.144
Grem2	2.62	0.0004	1.59	0.004
Smad1	−1.32	0.212	1.07	0.684
Smad2	1.05	0.035	1.14	0.013
Smad3	1.1	0.395	1.17	0.243
Smad4	1.05	0.169	1	0.501
Smad5	1.13	0.301	−1.03	0.404
Smad6	−1.3	0.124	−2.32	0.004
Smad7	1.46	0.014	−1.22	0.425
Smad8	−1.37	0.437	−3.06	0.006
Id1	1.27	0.317	−2.00	0.003
Id3	1.21	0.126	−2.01	0.002

Gene expression is reported as linear fold change, with *N*=3 samples per group, and *P*-value was calculated by one-way between-subject ANOVA for unpaired samples. Red text indicates BMP signaling response genes.

Table 2. Summary of microarray data assessing expression of genes in the Wnt signaling pathway in *Bmp2*$^{F/F}$ or *Bmp2*$^{Prx1\Delta/\Delta}$ cells treated with Wnt3a

Gene	Fold change (*Bmp2*$^{F/F}$ +Wnt3a vs *Bmp2*$^{F/F}$)	*P*-value (ANOVA, unpaired)	Fold change (*Bmp2*$^{Prx1\Delta/\Delta}$ +Wnt3a vs *Bmp2*$^{F/F}$ +Wnt3a)	*P*-value (ANOVA, unpaired)
Wnt2	1.06	0.669	−1.18	0.232
Wnt2b	1.07	0.348	1.02	0.506
Wnt3	1.09	0.224	−1.09	0.053
Wnt3a	1.05	0.356	−1.01	0.341
Wnt4	1.38	0.092	−1.78	0.001
Wnt5a	1.06	0.565	1.05	0.883
Wnt5b	−1.13	0.367	−1.09	0.024
Wnt6	1.1	0.213	−1.08	0.054
Wnt7a	−1.09	0.553	−1.1	0.164
Wnt7b	3.22	0.010	1.56	0.125
Wnt8a	−1.14	0.279	−1.09	0.269
Wnt9a	1.15	0.090	1.26	0.003
Wnt9b	1.15	0.160	−1.29	0.007
Wnt10a	−1.06	0.145	−1.07	0.013
Wnt10b	1.31	0.069	−1.33	0.071
Wnt11	1.09	0.565	−1.01	0.356
Wnt16	1.09	0.401	−1	0.850
Lrp4	−1.05	0.759	−2.85	0.011
Lrp5	−1.57	0.030	1.33	0.006
Lrp6	1.02	0.270	1.03	0.533
Rnf43	1.4	0.018	−1.22	0.358
Znf43	NR		−1.11	0.167
Lgr4	−1.37	0.145	1.00	0.978
Lgr5	1.64	0.129	6.42	0.0001
Lgr6	1.05	0.868	−2.54	0.003
Dkk1	−4.13	0.002	−1.11	0.99
Sost	1.14	0.867	−1.31	0.142
Notum	1.3	0.263	−4.27	0.002
Wif1	−1.02	0.971	−3.91	0.058
Frzb	−3.94	0.102	−1.66	0.193
Sfrp1	−2.71	0.009	1.21	0.049
Sfrp2	1.5	0.181	3.51	0.0002
Sfrp4	1.73	0.004	−1.13	0.384
Sfrp5	1.01	0.551	−1.05	0.185
Ctnnb1	−1.03	0.150	−1.02	0.126
Axin2	2.10	0.005	1.14	0.069

Gene expression is reported as linear fold change, with *N*=3 samples per group, and *P*–value was calculated by one-way between-subject ANOVA for unpaired samples. Red text indicates a Wnt signaling response gene.

staining, we found that *Bmp2*$^{Osx1\Delta/\Delta}$ cells are able to induce genes required for synthesis of mineralized bone matrix including *Col1a1*, *Alpl*, *Phospho1*, *Car3* and *Car12* (Fig. 5E).

Grainyhead-like 3 is a novel transcription factor in the osteoblast lineage that acts upstream of *Osx1* in a BMP2-dependent manner

We next investigated whether Grhl3 plays a role in osteoblast cell specification. To test if Grhl3 was sufficient to regulate osteoblast cell fate specification, we monitored specification of *Osx1*$^{+}$ cells in MLB13^{WT} or MLB13^{kdBmp2} cells transfected with human GRHL3. Immunoblot analysis showed that GRHL3 protein abundance is dramatically reduced by knockdown of *Bmp2* and enhanced by rBMP2. Canonical Wnt3a or Wnt10b had no effect on GRHL3 protein expression, alone or in combination with BMP2 (Fig. 6A). Although a longer stimulation period was required (>3 days) than in experiments in BMSCs, *Osx1* expression could be increased by treatment with Wnt3a or Wnt10b in MLB13^{WT} but not MLB13^{kdBmp2} cells, which expressed 20-times lower levels of *Osx1* than MLB13^{WT} (Fig. 6B). Strikingly, GRHL3 did not rescue the ability of Wnt3a or Wnt10b to induce *Osx*1 in MLB13^{kdBmp2} cells (Fig. 6B), but induced *Osx1* to levels indistinguishable from that of WT cells when expressed in the presence of rBMP2 (Fig. 6B). Ectopic expression of GRHL3 had minimal effects on *Dlx3* and *Dlx5* that did not correlate with specification of *Osx1*$^{+}$ cell phenotype (not shown). Importantly, different classes of cWnt ligands and antagonists bind distinct extracellular domains of Lrp5/6 (Bourhis et al., 2011; Gong et al., 2010); however, Wnt3a and Wnt10b had similar inhibitory effects on *Bmp2*-deficient cells.

To test if *Grhl3* was necessary for osteoblast differentiation, we monitored specification of *Osx1*$^{+}$ cell fate in MLB13^{WT} cells transfected with siRNAs targeting *Grhl3* (Fig. 6D). We also knocked down the highly conserved family member *Grhl2* (Fig. 6C) since it is expressed in our cell models, can heterodimerize with Grhl3 (Ting et al., 2003b) and has been shown to compensate for *Grhl3* during wound repair in skin (Boglev et al., 2011). Following knockdown, we stimulated cells for 48 h with BMP2, Wnt3a or BMP2+Wnt3a and then performed QPCR. Suppression of *Grhl3* resulted in a

Development (2016) 143, 4352-4367 doi:10.1242/dev.136879

Table 3. Summary of microarray data assessing expression of genes involved in endochondral ossification in *Bmp2*$^{F/F}$ or *Bmp2*$^{Prx1\Delta/\Delta}$ cells treated with Wnt3a

Gene	Fold change (*Bmp2*$^{F/F}$ +Wnt3a vs *Bmp2*$^{F/F}$)	*P*-value (ANOVA, unpaired)	Fold change (*Bmp2*$^{Prx1\Delta/\Delta}$ +Wnt3a vs *Bmp2*$^{F/F}$+Wnt3a)	*P*-value (ANOVA, unpaired)
Sox2	−1.02	0.660	−1.02	0.819
Nes	1.19	0.085	−1.08	0.225
Lepr	1.45	0.221	−2.33	0.078
Pdgfra	−1.85	0.007	−1.38	0.114
Prrx1	1.16	0.018	−1.01	0.310
Msx2	1.07	0.453	−1.08	0.228
Dermo1	−1.16	0.699	−1.09	0.819
Runx2	1.15	0.441	−1.28	0.490
Grhl3	2.55	0.034	−5.57	0.007
Osx1	−1.00	0.660	−2.89	0.038
Dlx1	−1.08	0.705	−1.17	0.020
Dlx2	1.55	0.102	−1.75	0.005
Dlx3	−1.61	0.078	−2.14	0.012
Dlx4	1.04	0.354	−1.11	0.083
Dlx5	−1.07	0.512	−1.93	0.025
Dlx6	−1.11	0.312	−1.46	0.015
Sox9	−1.09	0.516	−1.74	0.001
Mef2c	−1.15	0.199	−2.12	0.017
Ihh	1.2	0.439	−1.92	0.001
Ptch1	1.33	0.125	−2.37	0.033

Gene expression is reported as linear fold change, with *N*=3 samples per group, and *P*-value was calculated by one-way between-subject ANOVA for unpaired samples. Red text indicates differentially regulated transcription factors that affect endochondral lineages.

Table 4. Summary of microarray data assessing expression of genes involved in mineral metabolism in *Bmp2*$^{F/F}$ or *Bmp2*$^{Prx1\Delta/\Delta}$ cells treated with Wnt3a

Gene	Fold change (*Bmp2*$^{F/F}$ +Wnt3a vs *Bmp2*$^{F/F}$)	*P*-value (ANOVA, unpaired)	Fold change (*Bmp2*$^{Prx1\Delta/\Delta}$ +Wnt3a vs *Bmp2*$^{F/F}$+Wnt3a)	*P*-value (ANOVA, unpaired)
Alpl	−1.12	0.088	−1.91	0.041
Phospho1	−1.18	0.231	−2.44	0.045
Car1	1.08	0.300	−1.07	0.143
Car2	−1.56	0.157	−1.26	0.202
Car3	−1.16	0.745	−13.24	0.011
Car4	1.04	0.717	−1.2	0.453
Car5a	−1.12	0.147	−1.13	0.016
Car5b	−1.06	0.762	1.24	0.029
Car6	1.16	0.510	−1.28	0.068
Car7	1.13	0.401	−1.02	0.797
Car8	2.21	0.008	−1.77	0.0001
Car9	−1.14	0.182	−1.27	0.019
Car10	−1.03	0.565	−1.07	0.916
Car11	−1.1	0.119	−1.24	0.132
Car12	−3.2	0.164	−12.35	0.019
Car13	−1.01	0.850	1.09	0.301
Car14	−1.03	0.359	1	0.868
Car15	1.11	0.021	−1.03	0.339
Enpp1	1.05	0.436	−1.05	0.178
Mepe	−1.5	0.0006	−1.01	0.683
Phex	−4.14	0.022	−1.68	0.185
Dmp1	−1.64	0.238	−3.86	0.028

Gene expression is reported as linear fold change, with *N*=3 samples per group, and *P*-value was calculated by one-way between-subject ANOVA for unpaired samples. Red text indicates differentially regulated genes with potentially significant impact on biomineralization.

statistically significant though modest decrease in the abundance of *Prx1*, *Runx2*, *Dlx3* and *Dlx5* mRNAs expressed in BMP2 treated cells (Fig. 6E-H, red and black bars). Modest upregulation of *Prx1* by BMP2 was also blunted by suppression of *Grhl2* (Fig. 6E). As seen previously, BMP2 treatment led to high magnitude upregulation of *Osx1* and *Alpl* (45 and 20-fold, respectively), and this upregulation was blunted by 50-80% by introduction of *Grhl2* and/or *Grhl3* siRNAs (Fig. 6I,J). *Grhl3* siRNA also completely abrogated the induction of *Car12* by BMP2 (Fig. 6K). Expression of *Col1a1* and *Phospho1* were modestly reduced by *Grhl3* siRNAs (Fig. 6L,M). By contrast, *Car3* expression in response to Wnt3a greatly increased following suppression of *Grhl2* (Fig. 6N), consistent with the fact that Grhl proteins are Janus factors and can therefore act as transcriptional activators or repressors at different genetic loci. Moreover, *Grhl2* and *Grhl3* siRNAs did not cause a non-specific decrease in global gene expression. These cumulative results strongly suggest that Grhl2 and Grhl3 are both necessary and sufficient for the mechanism by which BMP2 specifies progenitors to an *Osx1*$^{+}$ osteoblast cell fate. Comprehensive statistical analysis is provided in Table S1.

Grhl3 is expressed during endochondral skeletal development and is induced during bone repair

Previous reports suggest *Grhl3* is expressed in the condensing limb bud mesenchyme of E13.5 mouse embryos (Kudryavtseva et al., 2003), consistent with our findings that *Grhl3* is expressed in E13.5 mouse limb bud cells. Consultation with the Eurexpress.org *in situ* hybridization database revealed that mRNAs for *Grhl3* are enriched in the perichondrium of developing endochondral structures in the E14.5 hindlimb (Fig. 7A,B), where the expression domain of *Grhl3* overlaps with *Lrp5* and *Bmp2* (Fig. 7C,D). *In situ* hybridization on E16.5 hindlimb and forelimb indicates *Grhl3* expression is evident in the developing bone collar, hypertrophic chondrocytes, and cells within the newly forming subchondral bone (Fig. 7E). This *Grhl3* expression domain corresponds to regions where newly forming osteoblasts appear during development (Salazar et al., 2016) and moreover, where Bmp2 is expressed when monitored using a *Bmp2*$^{ki(lacZ)}$ gene replacement allele (Fig. 7F). Finally, we created standardized fractures in adult mouse femurs to monitor *Grhl3* (and microarray hits) in an *in vivo* model of bone formation that relies on endogenous BMP2 and cWnt signaling mechanisms (Chen et al., 2007; Tsuji et al., 2006). QPCR analysis revealed that *Bmp2*, signaling molecules of the cWnt pathway, *Grhl2* and *Grhl3* continue to be expressed in marrow-free bone tissue in the adult skeleton (Fig. 7G,H). *Bmp2* and cWnt signaling molecules, as well as surrogate markers of BMP signaling (*Id3*) and Wnt signaling (*Axin2*) were robustly induced 5 days following fracture (Fig. 7G). These endogenous signaling dynamics characteristic of early endochondral bone repair were accompanied by no changes in *Grhl2*, a modest increase in *Runx2*, and striking inductions of *Prx1*, *Osx1* and *Grhl3* (Fig. 7H). *Car3*, *Car12*, *Alpl* and *Phospho1* were also induced at the fracture site (Fig. 7I), providing evidence that the molecular targets identified by microarray analysis in primary cells are biologically significant for osteoblast physiology during bone repair.

DISCUSSION

We used multiple mouse and primary cell models to test whether BMP and cWnt signaling play unique or redundant roles in the specification of new osteoblasts and subsequent production of bone matrix. Among the many BMPs expressed in bone, our data revealed a specific requirement for BMP2 in progression of *Prx1*$^{+}$ progenitors through the *Runx2/Osx1* transition. We identified Grhl3 as a

Development (2016) 143, 4352-4367 doi:10.1242/dev.136879

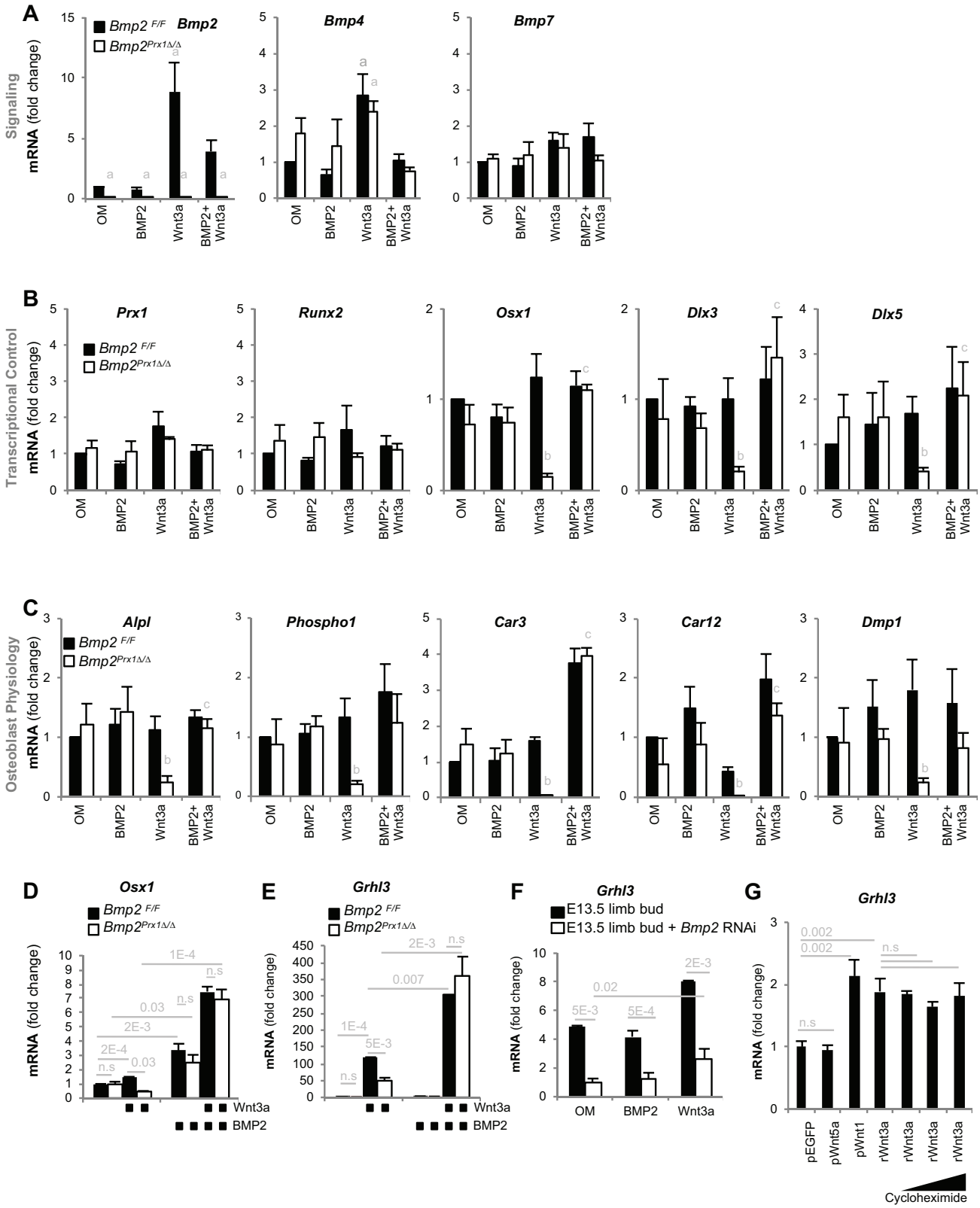

Fig. 4. Conditional ablation of *Bmp2* in the *Prx1*$^{+}$ lineage disrupts the *Runx2*/*Osx1* transition, mineral metabolism and upregulation of *Grhl3*. Primary BMSCs were differentiated in osteogenic medium (OM) plus growth factors. Cultures were performed in biological triplicates using pooled cells from n=3 $Bmp2^{F/F}$ or n=4 $Bmp2^{Prx1\Delta/\Delta}$ mice. QPCR on day 7 monitored expression of targets identified with microarray analysis, reported as mean±s.d. ^{a}P<0.05 vs $Bmp2^{F/F}$+OM, ^{b}P<0.05 vs $Bmp2^{F/F}$+Wnt3a, ^{c}P<0.05 vs $Bmp2^{Prx1\Delta/\Delta}$+Wnt3a. Genes were organized into: (A) BMP ligands, (B) transcriptional control of osteoblast differentiation, or (C) enzymes involved in formation of mineralized bone matrix. (D,E) QPCR for *Osx1* or *Grhl3* on primary unpooled BMSCs from n=3 $Bmp2^{Flox/Flox}$ and n=4 $Bmp2^{Prx1\Delta/\Delta}$ mice cultured for 72 h under osteogenic conditions with growth factors as indicated, expressed as mean±s.e.m. (F,G) QPCR for *Grhl3* expression in $MLB13^{WT}$ cells or $MLB13^{kdBmp2}$ cells, expressed as mean±s.d. relative to $MLB13^{WT}$ cells. N=3 biological replicates. n.s., not significant.

Development (2016) 143, 4352-4367 doi:10.1242/dev.136879

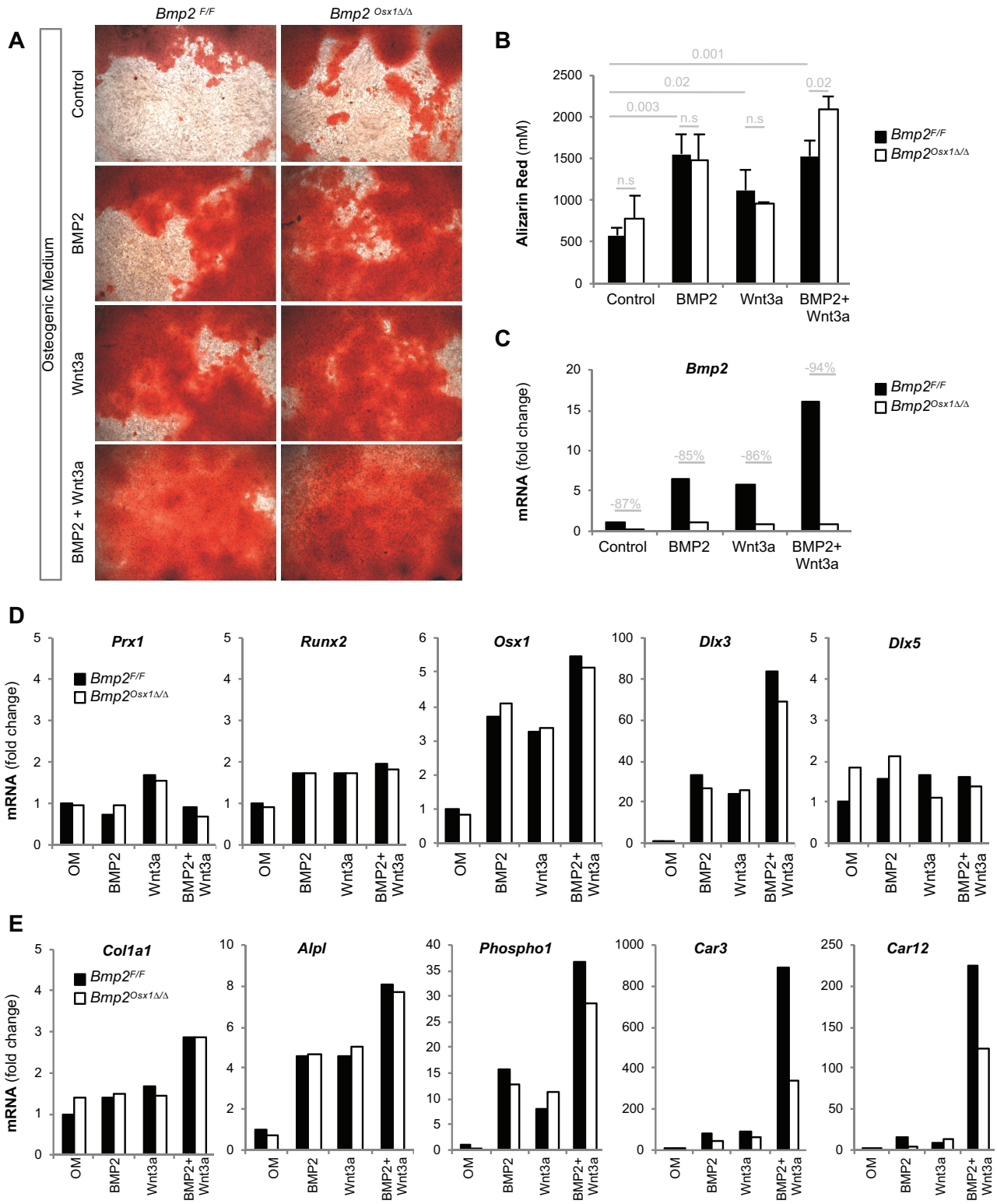

Fig. 5. BMSCs lacking *Bmp2* in the *Osx1*$^{+}$ lineage differentiate into mineralizing osteoblasts in response to cWnt signaling. Primary BMSCs from *Bmp2*$^{F/F}$ or *Bmp2; Osx1-Cre* (*Bmp2*$^{Osx1\Delta/\Delta}$) mice were differentiated in osteogenic medium (OM) plus growth factors. (A) Calcified matrix was assessed on day 10 by Alizarin Red staining (2.5×, bright field). Images represent biological triplicates using pooled cells from *n*=2 for *Bmp2*$^{F/F}$ and *Bmp2*$^{Osx1\Delta/\Delta}$ mice. (B) Quantification of Alizarin Red in A; mean±s.d. (C-E) QPCR analysis on single cultures harvested on day 7. n.s., not significant.

novel transcription factor in the osteoblast lineage that contributes to specification of an *Osx1*$^{+}$ cell fate in a BMP-dependent manner. These essential functions for BMP2 were enhanced by but not compensated for by cWnt activity in our primary cell model systems. We are currently completing a rigorous study of these findings *in vivo*.

The marrow and periosteum of adult bone provide essential niches for skeletal stem cells (Chan et al., 2015; Worthley et al., 2015) and

Development (2016) 143, 4352-4367 doi:10.1242/dev.136879

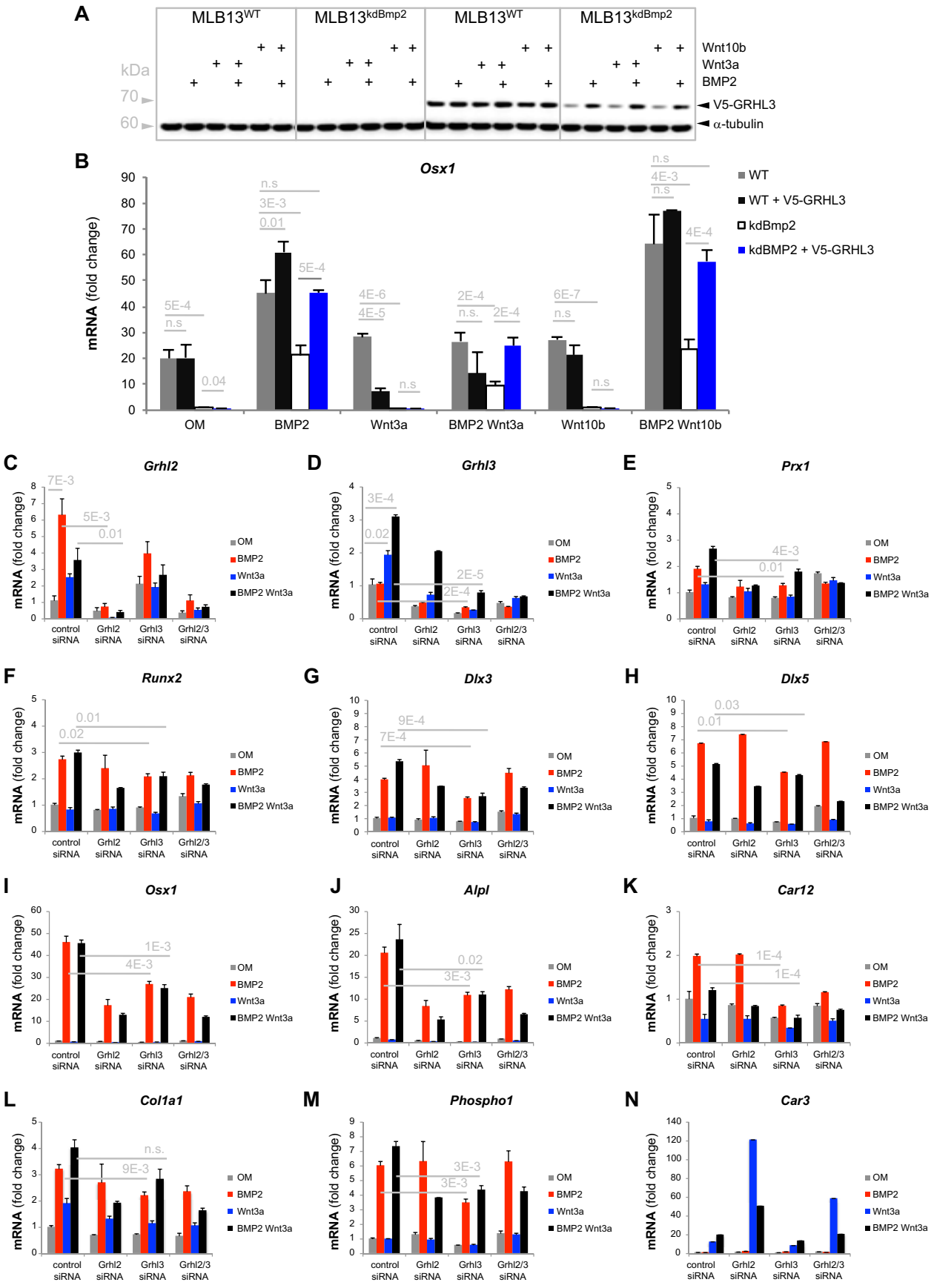

Fig. 6. See next page for legend.

Development (2016) 143, 4352-4367 doi:10.1242/dev.136879

Fig. 6. Grainyhead-like 3 (*Grhl3*) is a novel transcription factor that acts upstream of *Osx1* during osteoblast differentiation. (A) Immunoblot and (B) QPCR analysis on MLB13^{WT} or MLB13^{kdBmp2} cells expressing human GRHL3 with an N-terminal V5-tag and stimulated for 3 days with indicated ligands (+ indicates presence of ligand for each lane). Error bars represent s.d. of biological triplicates. Immunoblot shows cells expressing human V5-GRHL3. Similar results were obtained using human GRHL3-V5. (C-N) QPCR analysis on MLB13^{WT} cells, transfected with siRNA targeting mouse *Grhl2*, *Grhl3*, or *Grhl2* and *Grhl3*. Comprehensive statistical analysis provided in Table S1. n.s., not significant.

other fate-restricted skeletal progenitors (Mizoguchi et al., 2014; Ono et al., 2014; Zhou et al., 2014) that give rise to new osteoblasts for bone growth and repair during postnatal life (Kassem and Bianco, 2015; Kfoury and Scadden, 2015). Skeletal stem cells (SSCs) first appear in the limb bud mesenchyme, where *Prx1* is broadly expressed, and upon residency in adult bone, produce a variety of secreted niche factors including Bmp2, Wnt3a, TGFβ3 and Grem1 (Chan et al., 2015; Worthley et al., 2015; Yang et al., 2013). Accumulating data suggest that specific skeletal tissue types, such as bone or cartilage, can be induced from SSCs as well as ESCs (Craft et al., 2013) by controlling the timing and combination of growth factors presented to the cell. Understanding how each of these growth factors contributes, either alone or in combination, to a particular skeletogenic milieu has therefore emerged as a crucial step in understanding how to modulate bone mass or bone repair in humans with skeletal trauma or disease. The primary BMSC preparations used in this study expressed *Prx1*, *Lepr*, *Nes*, *Pdgfra* and *Grem1*, and therefore likely represent a heterogeneous population containing key skeletal progenitors identified in these recent studies. Of these markers, only *Lepr* was differentially expressed in *Bmp2*$^{Prx1\Delta/\Delta}$ cells. Future studies will shed light on whether BMP2 regulates the expression of *Lepr* and/or abundance of *Lepr*+ progenitors.

Here, we focused on understanding how BMP2 accomplishes transcriptional control of osteoblast differentiation from endochondral progenitors. *Bmp2*$^{Prx1\Delta/\Delta}$ cells successfully expressed transcriptional mediators of early endochondral bone formation including *Sox2*, *Hand2*, *Msx2*, *Prx1*, *Dermo1* and *Runx2*. However, *Bmp2*$^{Prx1\Delta/\Delta}$ cells expressed very low levels of late transcriptional mediators including *Dlx3*, *Dlx5* and *Osx1*, a group of proteins that heterodimerize to induce genes essential for the physiology of mature osteoblasts (Hojo et al., 2016). These data revealed a block in the *Runx2/Osx1* transition, consistent with the fact that *Osx1* was originally cloned as a BMP2-responsive gene (Nakashima et al., 2002). Importantly, however, *Osx1* expression is highly enriched in the skeleton and is therefore not indiscriminately expressed in all tissues undergoing active BMP signaling. We thus hypothesized that additional co-factors are required to target a BMP transcriptional response to the *Osx1* promoter during osteoblast differentiation. We focused on *Dlx3*, *Dlx5* and *Grhl3*, since microarray analysis indicated these were highly altered transcription factor genes in our samples. Since BMP2 is able to induce *Osx1* in cells lacking *Runx2* but not lacking *Dlx5* (Lee et al., 2003; Ulsamer et al., 2008), we used Ensembl to search 13 kb of the murine *Osx1* promoter for predicted Dlx binding motifs. Interestingly, we did not find Dlx3/5 binding sites, but did identify 12 predicted binding sites for Grhl3 intermingled with numerous Smad binding motifs (Gordon et al., 2014; Harrison et al., 2010).

We also found that Grhl3 is induced at the transcriptional level by cWnt signaling, and is regulated at the protein level by BMP2 signaling via as yet undefined mechanisms. Plasmid-based expression of GRHL3 specified *Osx1*$^{+}$ cell fate of limb bud progenitors in a BMP2-dependent and Wnt3a-independent manner, while suppression of *Grhl3* impaired the ability of BMP2 to induce *Osx1*. *In vivo* gene expression studies revealed that *Grhl3* is co-expressed in regions where BMP and cWnt signaling contribute to bone development and bone repair. *Grhl3* is therefore expressed at the appropriate time and place to be involved in developmental skeletogenesis and fracture repair. Our data strongly suggest that Grhl2 and Grhl3 play a necessary and sufficient role in the formation of *Osx1*$^{+}$ cells. Importantly, these collective findings reconcile with a requirement for both BMP and cWnt/β-catenin signaling during specification of *Osx1*$^{+}$ cells during skeletal development (Bandyopadhyay et al., 2006; Day et al., 2005; Hill et al., 2005). We are currently utilizing *in vivo* systems to evaluate Grhl3 as a potential nexus by which BMP2 and cWnt signaling cooperate to drive bone formation and bone repair *in vivo*. Further work is also needed to formally test the role of Grhl3 (and potential compensation by Grhl1 and Grhl2) in skeletal development.

A variety of human, mouse and fish studies suggest reduced expression of *Grhl3*, *Dlx3*, *Dlx5* and *Osx1* could explain the defects we found in calcium and phosphate metabolism (Dworkin et al., 2014; Han et al., 2011; Isaac et al., 2014; Lapunzina et al., 2010; Liu et al., 2015; Nguyen et al., 2013; Ting et al., 2003a). Mineralization of the endochondral skeleton is a complex biological process involving the formation of a calcium phosphate hydroxyapatite crystal that is deposited into an organic extracellular matrix composed primarily of type I collagen. Carbonic anhydrases (CAs) are zinc-dependent metalloenzymes that catalyze the hydration of carbon. Whereas in mammals, CAs are best known for their role in processing metabolic waste, regulating pH and fixing carbon, paleogenomic studies in sponges suggest that the ancestral CA was one of the first genes to confer the ability to synthesize skeletogenic structures through the formation of calcium carbonate (Jackson et al., 2007) and recent evidence suggests that calcium carbonate is an essential precursor crystal to the mature calcium phosphate hydroxyapatite crystals comprising endochondral bone (Müller et al., 2013). Although additional work clarifying the role of CA enzymes in bone metabolism is needed, we find that *Car3* and *Car12* are locally induced in bone following fracture.

In summary, we identify pre-*Osx1*$^{+}$ progenitors as a crucial source and target of endogenous BMP2 required for the *Runx2/Osx1* transition and show that BMP2 and cWnt play cooperative but non-redundant roles during osteoblast cell fate specification.

MATERIALS AND METHODS

Animals

In vivo experiments were performed in compliance with the Guide for the Care and Use of Laboratory Animals and were approved by the Harvard Medical Area Institutional Animal Care and Use Committee (protocol #04043 to V.R.). Mice carrying floxed *Bmp2* alleles (*Bmp2*$^{F/F}$) were bred to *Prx1-cre* mice (Logan et al., 2002) or *Osx1-cre* mice (Rodda and McMahon, 2006) to obtain *Bmp2*$^{F/F}$*; Prx1-Cre* mice (*Bmp2*$^{Prx1\Delta/\Delta}$) or *Bmp2*$^{F/F}$*; Osx1-EGFP::Cre* mice (*Bmp2*$^{Osx1\Delta/\Delta}$).

Standardized fractures

Standardized fractures with pin stabilization were made in femora of adult mice as previously described (Tsuji et al., 2006). Fractured and non-fractured contralateral controls femurs were collected 5 days post fracture and 6 mm of mid diaphysis bone were dissected, cleaned of bone marrow, snap frozen in liquid nitrogen, and processed for total RNA extraction according using Trizol and RNeasy Plus kit, as previously described (Salazar et al., 2013).

Cell culture

MLB13 cells were prepared from immortalized limb bud cells from E13.5 mouse embryos (MLB13 clone14) (Rosen et al., 1993, 1994) cultured and

Development (2016) 143, 4352-4367 doi:10.1242/dev.136879

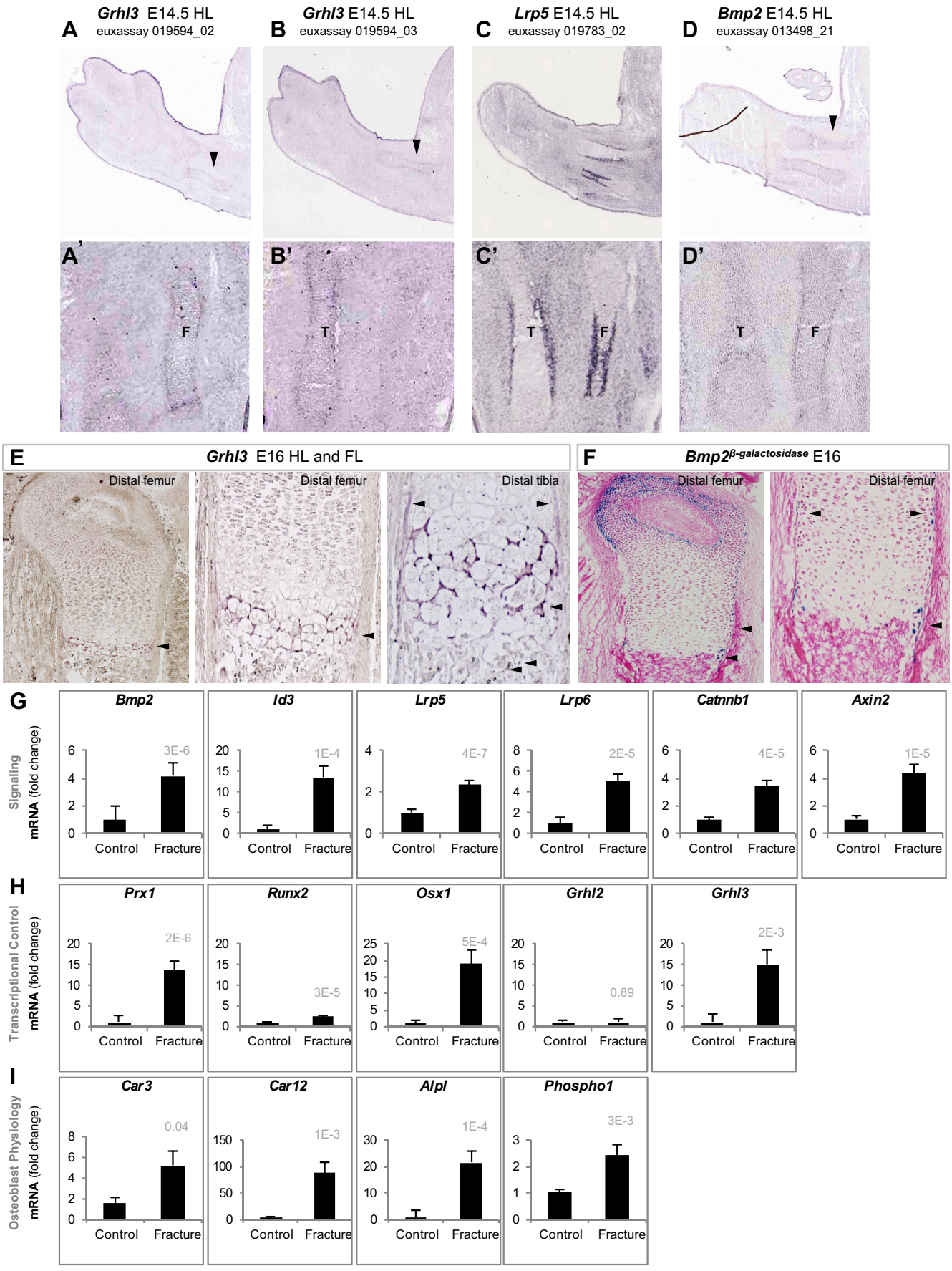

Fig. 7. See next page for legend.

Development (2016) 143, 4352-4367 doi:10.1242/dev.136879

Fig. 7. Grainyhead-like 3 (*Grhl3*) is expressed *in vivo* during bone development and bone repair. (A-D) *In situ* hybridization on E14.5 mouse hindlimb (HL). Arrowheads indicate mRNA expression in periochondrium of the presumptive femur and tibia. (A′-D′) Manual zoom of A-D, respectively. (E) *In situ* hybridization for *Grhl3*. (F) β-Galactosidase staining on limbs from E16 $Bmp2^{lacZ}$ knock-in mice. F, fibula; T, tibia. Arrowheads indicate enriched mRNA or β-galactosidase staining in the developing bone collar and the metaphyseal osteo/chondral border. (G-I) QPCR analysis on fractured or unfractured contralateral control femurs, expressed as mean±s.e.m. of *N*=6 bones per group.

maintained in DMEM supplemented with 10% fetal bovine serum and 100 U/ml penicillin-G and 100 mg/ml streptomycin. Cells are contamination free and were authenticated by neomycin resistance, which was conferred during immortalization. MLB13 cells were transfected with Bmp2-shRNA plasmid [BLOCK-iT, Invitrogen (5′-TGCTGAGTTCAAG-AA-GTCTCCAGCCAGTTTTG-GCCACTGACTGACTGG-CTGGACT-TCTTGAACT-3′)] using Lipofectamine 2000 (Invitrogen), selected for 3 weeks in 20 mg/ml blasticidin S and cloned by limiting dilution. Where indicated, cells were seeded to confluence and pretreated with cycloheximide (Sigma Aldrich, diluted to 25-100 mg/ml in growth medium) for 1 h prior to 4 h stimulation with Wnt3a+cyclohexamide.

BMSCs were prepared from bone marrow from 4- to 6-month-old mice (male and female) collected as previously described (Salazar et al., 2013) and plated in BMSC medium [ascorbic acid-free α-MEM (Invitrogen) containing 20% FBS, 40 mM L-glutamine, 100 U/ml penicillin-G and 100 mg/ml streptomycin]. After 3 days, non-adherent cells were removed by vigorous washing. For osteoblast differentiation, BMSCs were seeded in BMSC medium at 35,000 cells/well in 96-well dishes (for Alizarin Red staining) or 300,000 cells per well in 24-well dishes (for RNA or protein). Confluent cultures were stimulated on day 1 with osteogenic medium (OM: BMSC medium plus 50 µg/ml ascorbic acid and 10 mM β-glycerophosphate) and recombinant proteins.

Recombinant proteins were added as indicated to culture medium: human BMP2 (200 ng/ml; Genetics Institute), and mouse Wnt3a and Wnt10 (40 ng/ml; R&D Systems).

QPCR

Total RNA was harvested according to the manufacturer's instructions using the RNeasy Plus Kit (Qiagen). RNA was reverse transcribed with EcoDry Premix (Clontech). Data were normalized to β-actin, analyzed using the ΔΔCT method, and expressed as mean±s.d. (when biological replicates were established with pooled cells from multiple mice) or mean±s.e.m. (when biological replicates were established from unpooled cells from multiple mice) relative to $Bmp2^{F/F}$ cells cultured in osteogenic medium. Student's *t*-test was utilized to calculate *P*-values.

Alkaline phosphatase biochemical assay

Cells were plated at 2×10^4 cells/well in 96-well dishes, stimulated with Wnt3a for 3 days, fixed in acetone/ethanol (50:50), and incubated with a substrate solution composed of 0.1 M diethanolamine, 1 mM $MgCl_2$ and 1 mg/ml *p*-nitrophenylphosphate. The reaction was quenched with 3 M NaOH and absorbance measured at 405 nm.

Plasmids and siRNAs

Human GRHL3 plasmid was provided by the Center for Cancer Systems Biology, PlasmID clone HsCD00376192. MLB13 cells were seeded to 90% confluence, transfected with a plasmid encoding human GRHL3, and then cultured for 3 days in osteogenic medium plus indicated growth factors.

Cells were seeded 200K cells/well in a 24-well dish and transfected according manufacturer's directions using RNAiMax (Invitrogen) and 10 pmol of indicated siRNA. Cells were stimulated 48 h with osteogenic medium with or without BMP2 and Wnt3a or with BMP2+Wnt3a.

Adenovirus infection

Ad5-CMV-eGFP and Ad5-CMV-Cre-ires-eGFP viral particles were obtained from the University of Iowa Gene Transfer Vector Core. BMSCs were seeded at 40,000 cells/well in 96-well dishes for mineralization assays or 400,000 cells/well in 24-well dishes for QPCR, transduced for 6 h with 100 m.o.i of virus and 25 mM Hoechst in ascorbic acid-free α-MEM containing 2% FBS and L-glutamine, penicillin and streptomycin as for cell culture methods above. Cells recovered overnight in BMSC medium.

Histology

Cells were fixed 10 min in 10% neutral buffered formalin before staining with 1 mg Napthol AS-MX phosphate in 25 ml N,N-dimethylformamide plus 6 mg Fast Blue RR salt in 10 ml of buffer consisting of 0.1 M Tris-Base, 2 mM $MgCl_2$, pH 8.5.

For Alizarin Red staining, fixed cells were stained for 30 min in 0.4% aqueous solution of Alizarin Red S (Sigma). Alizarin Red S was eluted in 10% glacial acetic acid, pH was adjusted with 10% ammonium hydroxide, and absorbance measured at 405 nm.

Immunoblotting

Cells were scraped into RIPA buffer containing Halt protease and phosphatase inhibitors (Pierce) and homogenized with a QiaShredder column (Qiagen). Proteins were separated by SDS-page electrophoresis and immunoblotted with the following antibodies at 1:1000 dilution: p-Smad1/5 (Cell Signaling, 9511), p-Smad2/3 (Cell Signaling, 3101), β-catenin C-terminus (BD 61054), β-catenin N-terminus (Cell Signaling, 9562), osterix (Abcam, ab22552), V5 (Invitrogen, R961-25) and α-tubulin (Sigma, T6074).

Microarray analysis

Gene-level differential expression analysis was performed with Affymetrix Mouse ST 2.1 microarrays on BMSCs from $Bmp2^{F/F}$ or $Bmp2^{Prx1\Delta/\Delta}$ mice differentiated for 7 days with osteogenic medium alone or in medium plus BMP2 (100 ng/ml), Wnt3a (40 ng/ml) or both. Cultures were performed in biological triplicates using pooled cells from $n\geq3$ mice/genotype. Eight cDNA libraries were made from 100 ng total RNA using WT Expression Kit (Ambion): one pooled sample from three independent cultures of $Bmp2^{F/F}$ cells grown in osteogenic medium (33.33 ng each) or $Bmp2^{Prx1\Delta/\Delta}$ cells with BMP2+Wnt3a (33.33 ng each); three samples from three independent cultures of $Bmp2^{F/F}$ or $Bmp2^{Prx1\Delta/\Delta}$ cells with Wnt3a. Data were analyzed with Expression Console and Transcriptome Analysis Console v.3.0 (Affymetrix). Gene expression was reported as linear fold change relative to $Bmp2^{Prx1\Delta/\Delta}$ cells with Wnt3a, and *P*-values were calculated by one-way between-subject ANOVA for unpaired samples.

In situ hybridization and localization studies

E16 mouse embryo hindlimbs were fixed, paraffin processed and sectioned in the sagittal plane using standard methods. *In vitro* transcription to generate riboprobes was performed using standard protocols and reagents (Promega). *In situ* hybridization with digoxigenin-labeled *Grhl3* probe (kindly provided by Stephen Jane, Monash University, Australia) was carried out as described previously (Gamer et al., 2009). Hindlimbs from E16 mice were embedded in optimal cutting temperature compound (OCT) on dry ice and frozen sections were prepared for β-galactosidase staining as previously described (Kokabu et al., 2012).

Acknowledgements

We thank the University of Iowa Gene Transfer Vector Core (supported in part by the NIH and the Roy J. Career Foundation) for viral vectors; the Eurexpress.org ISH database for images of *Bmp2*, *Lrp5* and *Grhl3* expression; the Whitman lab for assembling V-5 tagged Grhl3 constructs; and Travis Burleson (Affymetrix) for microarray support.

Competing interests

The authors declare no competing or financial interests.

Author contributions

Conceptualization: V.S.S., L.C., V.R; Methodology: V.S.S., L.C., V.R.; Investigation: V.S.S., S.O., L.C., L.G.; Validation: S.O.; Formal analysis: V.S.S., S.O.; Data curation: V.S.; Funding acquisition: L.G., V.R.; Resources: V.R.; Writing – original draft: V.S.S.; Writing – review and editing: V.S.S., V.R.

Funding
This study was funded by the National Institute of Arthritis and Musculoskeletal and Skin Diseases (NIH-NIAMS) (R01 AR055904 to V.R.). Deposited in PMC for release after 12 months.

Data availability
Microarray data are deposited in Gene Expression Omnibus (GEO) under accession number GSE79377 (www.ncbi.nlm.nih.gov/geo/query/acc.cgi?acc=gse79377). Gene expression *in situ* hybridization images for *Grhl3*, *Lrp5* and *Bmp2* (shown in Fig. 7A-D′) are deposited in Eurexpress database under accession numbers 019594, 019783 and 013498, respectively.

Supplementary information
Supplementary information available online at
http://dev.biologists.org/lookup/doi/10.1242/dev.136879.supplemental

References
Bandyopadhyay, A., Tsuji, K., Cox, K., Harfe, B. D., Rosen, V. and Tabin, C. J. (2006). Genetic analysis of the roles of BMP2, BMP4, and BMP7 in limb patterning and skeletogenesis. *PLoS Genet.* **2**, e216.
Baron, R. and Kneissel, M. (2013). WNT signaling in bone homeostasis and disease: from human mutations to treatments. *Nat. Med.* **19**, 179-192.
Boglev, Y., Wilanowski, T., Caddy, J., Parekh, V., Auden, A., Darido, C., Hislop, N. R., Cangkrama, M., Ting, S. B. and Jane, S. M. (2011). The unique and cooperative roles of the Grainy head-like transcription factors in epidermal development reflect unexpected target gene specificity. *Dev. Biol.* **349**, 512-522.
Bourhis, E., Wang, W., Tam, C., Hwang, J., Zhang, Y., Spittler, D., Huang, O. W., Gong, Y., Estevez, A., Zilberleyb, I. et al. (2011). Wnt antagonists bind through a short peptide to the first beta-propeller domain of LRP5/6. *Structure* **19**, 1433-1442.
Boyden, L. M., Mao, J., Belsky, J., Mitzner, L., Farhi, A., Mitnick, M. A., Wu, D., Insogna, K. and Lifton, R. P. (2002). High bone density due to a mutation in LDL-receptor-related protein 5. *N. Engl. J. Med.* **346**, 1513-1521.
Cadigan, K. M. and Waterman, M. L. (2012). TCF/LEFs and Wnt signaling in the nucleus. *Cold Spring Harb. Perspect. Biol.* **4**, a007906.
Chan, C. K. F., Seo, E. Y., Chen, J. Y., Lo, D., McArdle, A., Sinha, R., Tevlin, R., Seita, J., Vincent-Tompkins, J., Wearda, T. et al. (2015). Identification and specification of the mouse skeletal stem cell. *Cell* **160**, 285-298.
Chappuis, V., Gamer, L., Cox, K., Lowery, J. W., Bosshardt, D. D. and Rosen, V. (2012). Periosteal BMP2 activity drives bone graft healing. *Bone* **51**, 800-809.
Chen, Y., Whetstone, H. C., Lin, A. C., Nadesan, P., Wei, Q., Poon, R. and Alman, B. A. (2007). Beta-catenin signaling plays a disparate role in different phases of fracture repair: implications for therapy to improve bone healing. *PLoS Med.* **4**, e249.
Craft, A. M., Ahmed, N., Rockel, J. S., Baht, G. S., Alman, B. A., Kandel, R. A., Grigoriadis, A. E. and Keller, G. M. (2013). Specification of chondrocytes and cartilage tissues from embryonic stem cells. *Development* **140**, 2597-2610.
Day, T. F., Guo, X., Garrett-Beal, L. and Yang, Y. (2005). Wnt/beta-catenin signaling in mesenchymal progenitors controls osteoblast and chondrocyte differentiation during vertebrate skeletogenesis. *Dev. Cell* **8**, 739-750.
Durland, J. L., Sferlazzo, M., Logan, M. and Burke, A. C. (2008). Visualizing the lateral somitic frontier in the Prx1Cre transgenic mouse. *J. Anat.* **212**, 590-602.
Dworkin, S., Simkin, J., Darido, C., Partridge, D. D., Georgy, S. R., Caddy, J., Wilanowski, T., Lieschke, G. J., Doggett, K., Heath, J. K. et al. (2014). Grainyhead-like 3 regulation of endothelin-1 in the pharyngeal endoderm is critical for growth and development of the craniofacial skeleton. *Mech. Dev.* **133**, 77-90.
Frietze, S., Wang, R., Yao, L., Tak, Y. G., Ye, Z., Gaddis, M., Witt, H., Farnham, P. J. and Jin, V. X. (2012). Cell type-specific binding patterns reveal that TCF7L2 can be tethered to the genome by association with GATA3. *Genome Biol.* **13**, R52.
Gamer, L. W., Cox, K., Carlo, J. M. and Rosen, V. (2009). Overexpression of BMP3 in the developing skeleton alters endochondral bone formation resulting in spontaneous rib fractures. *Dev. Dyn.* **238**, 2374-2381.
Gong, Y., Slee, R. B., Fukai, N., Rawadi, G., Roman-Roman, S., Reginato, A. M., Wang, H., Cundy, T., Glorieux, F. H., Lev, D. et al. (2001). LDL receptor-related protein 5 (LRP5) affects bone accrual and eye development. *Cell* **107**, 513-523.
Gong, Y., Bourhis, E., Chiu, C., Stawicki, S., DeAlmeida, V. I., Liu, B. Y., Phamluong, K., Cao, T. C., Carano, R. A. D., Ernst, J. A. et al. (2010). Wnt isoform-specific interactions with coreceptor specify inhibition or potentiation of signaling by LRP6 antibodies. *PLoS ONE* **5**, e12682.
Gordon, W. M., Zeller, M. D., Klein, R. H., Swindell, W. R., Ho, H., Espetia, F., Gudjonsson, J. E., Baldi, P. F. and Andersen, B. (2014). A GRHL3-regulated repair pathway suppresses immune-mediated epidermal hyperplasia. *J. Clin. Invest.* **124**, 5205-5218.
Guenther, C. A., Tasic, B., Luo, L., Bedell, M. A. and Kingsley, D. M. (2014). A molecular basis for classic blond hair color in Europeans. *Nat. Genet.* **46**, 748-752.
Han, Y., Mu, Y., Li, X., Xu, P., Tong, J., Liu, Z., Ma, T., Zeng, G., Yang, S., Du, J. et al. (2011). Grhl2 deficiency impairs otic development and hearing ability in a zebrafish model of the progressive dominant hearing loss DFNA28. *Hum. Mol. Genet.* **20**, 3213-3226.
Harrison, M. M., Botchan, M. R. and Cline, T. W. (2010). Grainyhead and Zelda compete for binding to the promoters of the earliest-expressed Drosophila genes. *Dev. Biol.* **345**, 248-255.
Hill, T. P., Später, D., Taketo, M. M., Birchmeier, W. and Hartmann, C. (2005). Canonical Wnt/beta-catenin signaling prevents osteoblasts from differentiating into chondrocytes. *Dev. Cell* **8**, 727-738.
Hojo, H., Ohba, S., He, X., Lai, L. P. and McMahon, A. P. (2016). Sp7/Osterix is restricted to bone-forming vertebrates where it acts as a Dlx co-factor in osteoblast specification. *Dev. Cell* **37**, 238-253.
Isaac, J., Erthal, J., Gordon, J., Duverger, O., Sun, H.-W., Lichtler, A. C., Stein, G. S., Lian, J. B. and Morasso, M. I. (2014). DLX3 regulates bone mass by targeting genes supporting osteoblast differentiation and mineral homeostasis in vivo. *Cell Death Differ.* **21**, 1365-1376.
Jackson, D. J., Macis, L., Reitner, J., Degnan, B. M. and Worheide, G. (2007). Sponge paleogenomics reveals an ancient role for carbonic anhydrase in skeletogenesis. *Science* **316**, 1893-1895.
Jho, E.-H., Zhang, T., Domon, C., Joo, C.-K., Freund, J.-N. and Costantini, F. (2002). Wnt/beta-catenin/Tcf signaling induces the transcription of Axin2, a negative regulator of the signaling pathway. *Mol. Cell. Biol.* **22**, 1172-1183.
Kassem, M. and Bianco, P. (2015). Skeletal stem cells in space and time. *Cell* **160**, 17-19.
Kent, W. J., Sugnet, C. W., Furey, T. S., Roskin, K. M., Pringle, T. H., Zahler, A. M. and Haussler, D. (2002). The human genome browser at UCSC. *Genome Res.* **12**, 996-1006.
Kfoury, Y. and Scadden, D. T. (2015). Mesenchymal cell contributions to the stem cell niche. *Cell Stem Cell* **16**, 239-253.
Kokabu, S., Gamer, L., Cox, K., Lowery, J., Tsuji, K., Raz, R., Economides, A., Katagiri, T. and Rosen, V. (2012). BMP3 suppresses osteoblast differentiation of bone marrow stromal cells via interaction with Acvr2b. *Mol. Endocrinol.* **26**, 87-94.
Kudryavtseva, E. I., Sugihara, T. M., Wang, N., Lasso, R. J., Gudnason, J. F., Lipkin, S. M. and Andersen, B. (2003). Identification and characterization of Grainyhead-like epithelial transactivator (GET-1), a novel mammalian Grainyhead-like factor. *Dev. Dyn.* **226**, 604-617.
Lapunzina, P., Aglan, M., Temtamy, S., Caparrós-Martin, J. A., Valencia, M., Letón, R., Martínez-Glez, V., Elhossini, R., Amr, K., Vilaboa, N. et al. (2010). Identification of a frameshift mutation in Osterix in a patient with recessive osteogenesis imperfecta. *Am. J. Hum. Genet.* **87**, 110-114.
Lee, M.-H., Kwon, T.-G., Park, H.-S., Wozney, J. M. and Ryoo, H.-M. (2003). BMP-2-induced Osterix expression is mediated by Dlx5 but is independent of Runx2. *Biochem. Biophys. Res. Commun.* **309**, 689-694.
Little, R. D., Folz, C., Manning, S. P., Swain, P. M., Zhao, S.-C., Eustace, B., Lappe, M. M., Spitzer, L., Zweier, S., Braunschweiger, K. et al. (2002). A mutation in the LDL receptor-related protein 5 gene results in the autosomal dominant high-bone-mass trait. *Am. J. Hum. Genet.* **70**, 11-19.
Liu, F., Yang, F., Wen, D., Xia, W., Hao, L., Hu, J. J., Zong, J., Shen, X., Ma, J., Jiang, N. et al. (2015). Grhl1 deficiency affects inner ear development in zebrafish. *Int. J. Dev. Biol.* **59**, 417-423.
Lo, K. W.-H., Ulery, B. D., Ashe, K. M. and Laurencin, C. T. (2012). Studies of bone morphogenetic protein-based surgical repair. *Adv. Drug Deliv. Rev.* **64**, 1277-1291.
Logan, M., Martin, J. F., Nagy, A., Lobe, C., Olson, E. N. and Tabin, C. J. (2002). Expression of Cre Recombinase in the developing mouse limb bud driven by a Prxl enhancer. *Genesis* **33**, 77-80.
Mizoguchi, T., Pinho, S., Ahmed, J., Kunisaki, Y., Hanoun, M., Mendelson, A., Ono, N., Kronenberg, H. M. and Frenette, P. S. (2014). Osterix marks distinct waves of primitive and definitive stromal progenitors during bone marrow development. *Dev. Cell* **29**, 340-349.
Müller, W. E. G., Schröder, H. C., Schlossmacher, U., Grebenjuk, V. A., Ushijima, H. and Wang, X. (2013). Induction of carbonic anhydrase in SaOS-2 cells, exposed to bicarbonate and consequences for calcium phosphate crystal formation. *Biomaterials* **34**, 8671-8680.
Nakashima, K., Zhou, X., Kunkel, G., Zhang, Z., Deng, J. M., Behringer, R. R. and de Crombrugghe, B. (2002). The novel zinc finger-containing transcription factor osterix is required for osteoblast differentiation and bone formation. *Cell* **108**, 17-29.
Nguyen, T., Phillips, C., Frazier-Bower, S. and Wright, T. (2013). Craniofacial variations in the tricho-dento-osseous syndrome. *Clin. Genet.* **83**, 375-379.
Ono, N., Ono, W., Nagasawa, T. and Kronenberg, H. M. (2014). A subset of chondrogenic cells provides early mesenchymal progenitors in growing bones. *Nat. Cell Biol.* **16**, 1157-1167.
Rodda, S. J. and McMahon, A. P. (2006). Distinct roles for Hedgehog and canonical Wnt signaling in specification, differentiation and maintenance of osteoblast progenitors. *Development* **133**, 3231-3244.
Rosen, V., Capparella, J., McQuaid, D., Cox, K., Thies, R. S., Song, J. and Wozney, J. (1993). Development of immortalized cells derived from 13DPC mouse limb buds as a system to study the effects of recombinant human bone morphogenetic protein-2 (rhBMP-2) on limb bud cell differentiation. *Prog. Clin. Biol. Res.* **383A**, 305-315.

Rosen, V., Nove, J., Song, J. J., Thies, R. S., Cox, K. and Wozney, J. M. (1994). Responsiveness of clonal limb bud cell lines to bone morphogenetic protein 2 reveals a sequential relationship between cartilage and bone cell phenotypes. *J. Bone Miner. Res.* **9**, 1759-1768.

Rowe, P. S. N. (2012). Regulation of bone-renal mineral and energy metabolism: the PHEX, FGF23, DMP1, MEPE ASARM pathway. *Crit. Rev. Eukaryot. Gene Expr.* **22**, 61-86.

Salazar, V. S., Zarkadis, N., Huang, L., Norris, J., Grimston, S. K., Mbalaviele, G. and Civitelli, R. (2013). Embryonic ablation of osteoblast Smad4 interrupts matrix synthesis in response to canonical Wnt signaling and causes an osteogenesis-imperfecta-like phenotype. *J. Cell Sci.* **126**, 4974-4984.

Salazar, V. S., Gamer, L. W. and Rosen, V. (2016). BMP signalling in skeletal development, disease and repair. *Nat. Rev. Endocrinol.* **12**, 203-221.

Shore, E. M., Xu, M., Feldman, G. J., Fenstermacher, D. A., Cho, T. J., Choi, I. H., Connor, J. M., Delai, P., Glaser, D. L., LeMerrer, M. et al. (2006). A recurrent mutation in the BMP type I receptor ACVR1 causes inherited and sporadic fibrodysplasia ossificans progressiva. *Nat. Genet.* **38**, 525-527.

Shu, W., Guttentag, S., Wang, Z., Andl, T., Ballard, P., Lu, M. M., Piccolo, S., Birchmeier, W., Whitsett, J. A., Millar, S. E. et al. (2005). Wnt/beta-catenin signaling acts upstream of N-myc, BMP4, and FGF signaling to regulate proximal-distal patterning in the lung. *Dev. Biol.* **283**, 226-239.

Ting, S. B., Wilanowski, T., Auden, A., Hall, M., Voss, A. K., Thomas, T., Parekh, V., Cunningham, J. M. and Jane, S. M. (2003a). Inositol- and folate-resistant neural tube defects in mice lacking the epithelial-specific factor Grhl-3. *Nat. Med.* **9**, 1513-1519.

Ting, S. B., Wilanowski, T., Cerruti, L., Zhao, L.-L., Cunningham, J. M. and Jane, S. M. (2003b). The identification and characterization of human Sister-of-Mammalian Grainyhead (SOM) expands the grainyhead-like family of developmental transcription factors. *Biochem. J.* **370**, 953-962.

Tsuji, K., Bandyopadhyay, A., Harfe, B. D., Cox, K., Kakar, S., Gerstenfeld, L., Einhorn, T., Tabin, C. J. and Rosen, V. (2006). BMP2 activity, although dispensable for bone formation, is required for the initiation of fracture healing. *Nat. Genet.* **38**, 1424-1429.

Ulsamer, A., Ortuno, M. J., Ruiz, S., Susperregui, A. R. G., Osses, N., Rosa, J. L. and Ventura, F. (2008). BMP-2 induces Osterix expression through up-regulation of Dlx5 and its phosphorylation by p38. *J. Biol. Chem.* **283**, 3816-3826.

Waby, J. S., Bingle, C. D. and Corfe, B. M. (2008). Post-translational control of sp-family transcription factors. *Curr. Genomics* **9**, 301-311.

Wang, X., Schröder, H. C., Schlossmacher, U., Neufurth, M., Feng, Q., Diehl-Seifert, B. and Müller, W. E. G. (2014). Modulation of the initial mineralization process of SaOS-2 cells by carbonic anhydrase activators and polyphosphate. *Calcif. Tissue Int.* **94**, 495-509.

Worthley, D. L., Churchill, M., Compton, J. T., Tailor, Y., Rao, M., Si, Y., Levin, D., Schwartz, M. G., Uygur, A., Hayakawa, Y. et al. (2015). Gremlin 1 identifies a skeletal stem cell with bone, cartilage, and reticular stromal potential. *Cell* **160**, 269-284.

Yadav, M. C., Simão, A. M. S., Narisawa, S., Huesa, C., McKee, M. D., Farquharson, C. and Millán, J. L. (2011). Loss of skeletal mineralization by the simultaneous ablation of PHOSPHO1 and alkaline phosphatase function: a unified model of the mechanisms of initiation of skeletal calcification. *J. Bone Miner. Res.* **26**, 286-297.

Yang, W., Guo, D., Harris, M. A., Cui, Y., Gluhak-Heinrich, J., Wu, J., Chen, X.-D., Skinner, C., Nyman, J. S., Edwards, J. R. et al. (2013). Bmp2 in osteoblasts of periosteum and trabecular bone links bone formation to vascularization and mesenchymal stem cells. *J. Cell Sci.* **126**, 4085-4098.

Zhang, R., Oyajobi, B. O., Harris, S. E., Chen, D., Tsao, C., Deng, H.-W. and Zhao, M. (2013). Wnt/beta-catenin signaling activates bone morphogenetic protein 2 expression in osteoblasts. *Bone* **52**, 145-156.

Zhou, B. O., Yue, R., Murphy, M. M., Peyer, J. G. and Morrison, S. J. (2014). Leptin-receptor-expressing mesenchymal stromal cells represent the main source of bone formed by adult bone marrow. *Cell Stem Cell* **15**, 154-168.